
UNSTABLE RESONATOR SEMICONDUCTOR LASERS BELOW THRESHOLD

Yurii Anan'ev
Ted Salvi
Dave Depatie

October 1996

Final Report

19970113 120

APPROVED FOR PUBLIC RELEASE; DISTRIBUTION IS UNLIMITED.



PHILLIPS LABORATORY
Lasers and Imaging Directorate
AIR FORCE MATERIEL COMMAND
KIRTLAND AIR FORCE BASE, NM 87117-5776

Using Government drawings, specifications, or other data included in this document for any purpose other than Government procurement does not in any way obligate the U.S. Government. The fact that the Government formulated or supplied the drawings, specifications, or other data, does not license the holder or any other person or corporation; or convey any rights or permission to manufacture, use, or sell any patented invention that may relate to them.

This report has been reviewed by the Public Affairs Office and is releasable to the National Technical Information Service (NTIS). At NTIS, it will be available to the general public, including foreign nationals.

If you change your address, wish to be removed from this mailing list, or your organization no longer employs the addressee, please notify PL/LIDA, 3550 Aberdeen Ave SE, Kirtland AFB, NM 87117-5776.

Do not return copies of this report unless contractual obligations or notice on a specific document requires its return.

This report has been approved for publication.

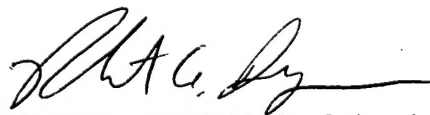


DAVID DEPATIE
Project Manager

FOR THE COMMANDER



MICHAEL R. GREGG, CAPT, USAF
Acting Chief, Semiconductor Laser Branch



ROBERT A. DURYEA, Colonel, USAF
Director, Lasers and Imaging Directorate

DRAFT SF 298

1. Report Date (dd-mm-yy) 8-10-96		2. Report Type FINAL		3. Dates covered (from... to) 28 FEB 94 - 10 OCT 96	
4. Title & subtitle UNSTABLE RESONATOR SEMICONDUCTOR LASERS BELOW THRESHOLD				5a. Contract or Grant #	
				5b. Program Element # 61101F	
6. Author(s) Yurii Anan'ev Ted Salvi Dave Depatie				5c. Project # 1L1R	
				5d. Task # LC	
				5e. Work Unit # 01	
7. Performing Organization Name & Address Phillips Laboratory 3550 Aberdeen Ave SE Kirtland AFB, NM 87117-5776				8. Performing Organization Report # PL-TR-96-1159	
9. Sponsoring/Monitoring Agency Name & Address				10. Monitor Acronym LIDA	
				11. Monitor Report #	
12. Distribution/Availability Statement Approved for Public Release; Distribution is Unlimited					
13. Supplementary Notes					
14. Abstract This report documents an investigation of the unique spontaneous emission patterns observed from two-dimensional unstable resonators fabricated on semiconductor diode lasers. Both geometrical and modal analysis lead to similar conclusions: these quasi-modes below threshold may be useful in manufacturing diagnostics, but have little influence on the behavior of laser (above threshold) operation.					
15. Subject Terms Lasers, unstable resonator, below threshold, semiconductor diode					
Security Classification of			19. Limitation of Abstract Unlimited	20. # of Pages 60	21. Responsible Person (Name and Telephone #) Dr David Depatie 505-846-5879
16. Report Unclassified	17. Abstract Unclassified	18. This Page Unclassified			

Preface

This report is the result of the fall of the Soviet Empire and the realization by the USAF that the opportunity to obtain excellent technology and also support Russian scientists was in US interest. In response to requests to initiate promising contacts, Ted Salvi of Phillips Laboratory, acted on a suggestion from Prof Tony Siegman and invited Dr Yurii Anan'ev to visit. Prof Siegman had met a number of prominent Soviet scientist in St Petersburg in 1991 and understood Phillips Laboratory interests. These three scientists are united by their interest in and contributions to laser optics, particularly unstable resonators. Prof Siegman wrote an introduction to Dr Anan'ev's book, "Laser Resonators and the Beam Divergence Problem," which should be consulted for historical context.

The government to government invitation finally succeeded, due in part to the exceptional enterprise of Ted Salvi, and a month long visit to the US was arranged. Dr Anan'ev (he writes his name in english as Ananiev) and his wife, Tatania, came to Albuquerque and Phillips Laboratory the week of January 11, 1993, and lectured at PL/LIDA, the IEEE Lasers and Electro-optics Society meeting, and at the University of New Mexico. Ted Salvi was host for this unprecedented visit.

Following his return to St Petersburg, Russia, Phillips Laboratory made funds available through the ILIR (In-house Laboratory Independent Research) program for a small research effort. An appropriate problem had been identified, and a contract with Dr Anan'ev and associates at the Laser Technology Center, St Petersburg State Technical University, was established. This report documents that effort.

The extensive contributions of Harro Ackermann, Greg Dente, and Charles Moeller to this project are gratefully acknowledged. Visit support was contributed by PL, SPIE, HDOS, TRW, Rofin Sinar (Seimans) and LEOS.

Contents

Preface	iv
Chapter 1: Introduction	1
Chapter 2: Anan'ev's First report, 28 Oct 94	3
"Explanation of Behavior of Semiconductor Laser with Unstable Resonator in Sub-threshold Regime"	
Chapter 3: Anan'ev's Interim Report, 9 Mar 95	7
"Additional Considerations on the Behavior of Semiconductor Lasers with Unstable Resonators operated in the Sub-threshold Regime"	
Chapter 4: Anan'ev's Last Report, 17 Jul 95	13
"Considerations about Summary 'ASE Patterns & Mode Formation in Unstable Resonators' of Dente, <i>et al</i> and ..."	
Chapter 5: Conclusions	27
Appendix: "ASE Patterns & Mode Formation in Unstable Resonators"	29

US Authors' note:

Dr Anan'ev's reports were sent from Russia by fax, the most reasonable means at that time. Even though the quality of the facsimile is low, to insure accuracy we have chosen to reproduce the reports as received, with the source material sent to Russia as an Appendix, and a short introduction and summary. The responsibility for this additional material rests entirely with the US authors.

1. INTRODUCTION

Unstable Resonators Driven by Spontaneous Emission

A curious phenomenon was discovered in unstable resonators in diode lasers in 1992 and 1993. The spectrally dispersed near field of the output of an unstable resonator diode laser pumped just below lasing threshold was observed using a grating spectrometer. This is possible because diode lasers are essentially one dimensional emitters, the transverse direction (growth direction) is a very narrow single mode waveguide. An unstable resonator can be created in the lateral direction by several methods, and an active research effort has been underway. The startling data that were taken when the resonator was just below threshold displayed a herringbone-like pattern with anomalous curvature. The mode¹ at each frequency seems to have two major bumps, which change continuously as a function of frequency. The modes are below threshold, but spontaneous emission at each frequency is preferentially amplified in the modes seen. A paper was published in Electronics Letters² in September 1993 that showed the phenomenon. Greg Dente³ did several types of analysis, all of which are intriguing but are difficult to tie together in a coherent picture. He gave a talk at the January 1994 Winter Colloquium on Quantum Electronics in Snowbird, Utah on the subject. Excerpts from the paper and viewgraphs⁴ from the talk are included in this report.

¹ Modes of unstable resonators are not proper mathematical modes as noted by Anan'ev in paragraph 2 of his first (interim) report. These 'quasi-modes' are useful concepts, however, and will be referred to as modes in this report.

² Bao et al., Electronics Letters, 29, pp1597-1598, (Sep 93)

³ Dente and Tilton, PL-TR-94-1061, pp 92-103.

⁴ Unpublished

The most dramatic attribute of the data was the direction of the curvature of the patterns. This curvature is opposite of the patterns observed in Fabry-Perot lasers. The curvature in Fabry-Perot lasers is easily understood by requiring that the z component of the propagation constant, k_z , remains fixed for each longitudinal mode ($k_z L/\pi$ is the longitudinal integer mode index), and arbitrary k_y provides the shape of the curves. In the farfield, the higher spatial frequencies have higher total k and thus shorter wavelength. The curvature reverses for the unstable resonator lasers.

The data raise fundamental questions about the existence and nature of spontaneous-emission-driven higher loss modes in a running resonator, and about the mechanism at work during the turn-on of an unstable resonator. Professor Anan'ev was the ideal person to work on this problem. He is a pioneer in laser unstable resonators, and his book⁵ is a classic in the field. He had also been somewhat exiled in his own country for the last two decades, having been 'purged' from the USSR military research programs. Last year, one visiting Russian graduate student said that Anan'ev was a 'legendary figure' in Russia and that his book was hard to obtain there. We felt we would all benefit by working together on a problem so basic to laser operation which might also shed light on the fundamental limitations to coherent laser performance.

The reports provided by Professor Anan'ev are difficult to read. This is partly due to the nature of the subject and partly due to language difficulties. To make this report more readable, we have added some background material: a Preface, this first chapter, an Appendix containing Dente's Viewgraphs that were sent to Russia, and a summary chapter. The second chapter is the original report made by Professor Anan'ev: An interim report provided in October 1994. In March 1995, another report was submitted, with a computer code which calculates the onset of lasing in a resonator, (Chapter 3). Final comments, Chapter 4, were provided in July 1995. The final chapter is a summary of conclusions on the topic.

⁵ Yu Anan'ev, *Laser Resonators and the Beam Divergence Problem*, Adam Hilger, Bristol, Philadelphia and New York, 1992.

EXPLANATION OF BEHAVIOUR OF SEMICONDUCTOR LASER WITH UNSTABLE RESONATOR IN SUB-THRESHOLD REGIME (INTERIM REPORT)

1. Experimental data

The experimental data concerning a properties of diode laser behaviour in sub-threshold regime and having been informed by Phillips Lab are as follows.

The observations have uncovered an unusual property in the output of unstable resonators. It is possible to spectrally disperse the near field output of an unstable resonator diode laser by using a grating spectrometer. Since diode lasers are essentially one dimensional emitters, the transverse direction (growth direction) is a very narrow single mode waveguide. An unstable resonator can be created in the lateral direction by several methods. The interesting laboratory data was obtained when the resonator was just below threshold. It consisted of a pattern similar to a herringbone. The mode at each frequency appears to have two major bumps, which change continuously as a function of frequency. The modes are below threshold, but spontaneous emission at each frequency is preferentially amplified in the observed modes. Besides this information, there are many photos of spectrally resolved near-field distribution of diode-laser radiation in sub-threshold regime.

2. About possibilities of phenomena description by idea of unstable resonator modes

It is well-known that if for two neighbouring resonance frequencies of a system, $\omega_1 = \omega'_1 - i\omega''_1$ and $\omega_2 = \omega'_2 - i\omega''_2$ (the timefactor of the complex-valued amplitude is $\exp(-i\omega t)$), the following inequality is valid

$$2 |\omega'_1 - \omega'_2| / (\omega''_1 + \omega''_2) < 1 \quad (1)$$

then their resonance curves overlap (see, for example, [1]). Let us make corresponding evaluation for the first and the second modes of a plane resonator with the same overall dimensions and sum losses of radiation per double transit as is the case of diode-laser unstable resonator.

Using the notation of [1], section 3.1, we have $2 |\omega'_1 - \omega'_2| / (\omega''_1 + \omega''_2) = 4 |\delta'_1 - \delta'_2| / (\Delta_1 + \Delta_2)$ where δ'_m are phase corrections and Δ_m are the relative losses of radiation intensity per double transit. For the plane resonator modes $\delta'_m \approx \frac{\pi}{8N} (m+1)^2$ where N is Fresnel number and m is transverse index.

Therefore $|\delta'_0 - \delta'_1| \approx \frac{3\pi}{8N}$; for conditions when resonator is filled by medium with refractive coefficient n , $N = a^2 n / \lambda L_0$, where a is the half width, λ - wave length in vacuum, and L_0 - the length of resonator. In our case $\lambda = 0.97 \text{ } \mu\text{m}$, $a = 100 \text{ } \mu\text{m}$, $L_0 = 500 \text{ } \mu\text{m}$, thus $N \approx 72$ and $|\delta'_0 - \delta'_1| \approx 0.017$. Because of larger width of beams in unstable resonators the phase corrections in this case are still smaller. At the same time the losses of radiation per double transit even in condition of their partially compensation by gain in sub-threshold regime turn out much higher. In actual fact, threshold gain per double bounce is equal here $M/R' \approx 7.8$ where R' is the Fresnel reflection coefficient. If intensity of the excitation is lower than threshold one only at 5%, the gain is equal $7.8^{0.95} \approx 7.0$, and the relative losses for the first mode of unstable resonator are $(7.8 - 7.0) / 7.8 \approx 10\%$; for the second one they are dramatically higher. We can conclude that condition (1) is obviously valid and unstable resonator mode structure cannot be observed.

The unstable resonator modes cannot be used also for series expansion of arbitrary light field: eigenfunctions of unstable resonator do not make up a complete orthonormalized set, so that one cannot use such an expansion [2, 1]. Therefore we are forced to give up attempts of use an information about resonator modes and transfer to methods of classical optics.

3. Explanation of phenomena experimentally observed from the viewpoint of classical optics

The law that describes the spatially-spectral pattern is similar to the one for fringes of equal thickness [3]. To evaluate this dependence, you have to find out the distance $L(x)$ from plane mirror to the convex one. This distance has to be calculated along the way parallel to the axis and remote from it at x (see Figure). It's easy to find that

$$L(x) = L_0 + \frac{x^2}{2R} \quad (2)$$

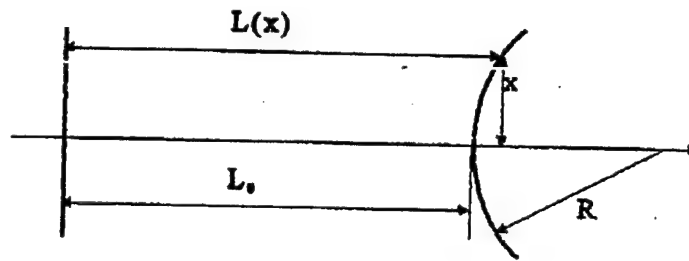
where radius $R = \frac{4M}{(M-1)^2} \cdot L_0 \approx 2200 \text{ } \mu\text{m}$ ($M = 2.5$ - magnification coefficient of resonator).

The interference at the axis takes place for wavelength λ_q :

$$L_0 \cdot n = m \cdot \frac{\lambda_m}{2} \quad (3)$$

where n - index of refraction, q - the order of interference.

The same expression can be written for the points with $x \neq 0$



$$L(x) \cdot n = m \frac{\lambda_m + \Delta\lambda_m(x)}{2} \quad (4)$$

and therefore

$$\Delta\lambda_m(x) = \frac{x^2 \cdot n}{R \cdot m} \approx \frac{x^2}{2RL_0} \cdot \lambda \quad (5)$$

One can attach the index "q" to this parabola. The experimental spatially-spectral pattern is the sequence of precisely these such parabolas. Their spectral distance at the axis is

$$\delta\lambda = \frac{\lambda^2}{2L_0 n} \approx 4\lambda \quad (6)$$

A straight line corresponding to any λ intersects the sequence of parabolas in the points, forming the succession of interference peaks.

Thus the shape and position of spots experimentally observed can be explained by the idea of fringes of equal thickness.

4. About spectral and spatial width of pattern

In this section we shall discuss factors defining the width and number of "arcs" on spectral-resolved distributions which are observed experimentally. We don't know any works considering interferometers with medium which emits and amplifies a light in sub-threshold regime. An interference pattern must be clear if an elementary wave is passing at least two times through the same place and has approximately the same amplitude. Let us use this assumption.

a) Overall spectral width of experimental pattern.

We see primarily that the spectral width observed is several times smaller than one of luminescence line. The explanation is very simple: we saw that the gain coefficient drops rapidly as frequency moves away from the centre of luminescence line. Concurrently the wave intensity after two bounces drops also, and interference pattern does not keep existing.

b) Spatial width of interference pattern.

Let us consider the conditions of interference pattern existence when angle between mirrors is α .

We can consider that our elementary wave moves after two bounces on the same trajectory only if condition $\alpha_d \approx \lambda/hn$, or

$$h \leq \lambda/\alpha n \quad (7)$$

is valid, where α_d is diffraction angle and h is the size along the wave front. On the other hand, in order to avoid significant losses, α_d should be not excessively big, and condition $L_0\alpha_d \leq h$, or

$$h^2 \geq 2L_0\lambda/n \quad (8)$$

must be valid.

We can easily see that (7) and (8) can be valid simultaneously if $\alpha \leq \sqrt{\lambda/2L_0n}$. For magnitude a_0 of the half-width of zone where angle between mirrors of our resonator is smaller than α we find $a_0 \leq \alpha_0 R \approx 35 \mu m$. Taking into account the rough of evaluation, we can conclude that this value corresponds to the experimental data quite satisfactorily.

5. Conclusion

The results of the above-provided calculations permit to conclude that the phenomena model offered by us has explained qualitatively all experimental data.

References

1. Yu. Anan'ev. Laser Resonators and the Beam Divergence Problem.- Adam Hilger, Bristol, Philadelphia and New York, 1992
2. Yu. A. Anan'ev, S. G. Anikichev. -*Optika i spektroskopiya* v. 61, p. 856, 1986
3. M. Born, E. Wolf. Principles of optics. Pergamon Press, 1964

Head of the project



Y. Ananiev

ADDITIONAL CONSIDERATIONS ON THE BEHAVIOR OF
 SEMICONDUCTOR LASERS WITH UNSTABLE RESONATORS
 OPERATED IN THE SUB-THRESHOLD REGIME,
 AND A PRELIMINARY DESCRIPTION OF A COMPUTER PROGRAM
 FOR CALCULATING THE TRANSITION OF AN UNSTABLE-RESONATOR
 LASER FROM SUB-THRESHOLD OPERATION TO LASING
 (DETAILED PROGRAM STATUS REPORT)

This report presents some additional considerations concerning the problem of radiation coherence in sub-threshold regime, which was not dealt with in the preceding interim report. ~~Since it is the~~ *subthreshold* regime where the lasing starts from, we believed it appropriate to study in more detail this process, and to develop the corresponding computational technique applicable to lasers with unstable resonators.

1. On the Problem of Radiation Coherence in Sub-Threshold Regime

The preceding report described the observed pattern of radiation intensity spectral distribution over the resonator output mirror in terms of classical optics; in more than one respect it is similar to a many-color picture produced by illuminating a thin film with white light. There is, however, a substantial difference associated with the significance of mutual coherence of the primary radiation sources.

Indeed, in the case of thin films we deal with an illumination source located on one side of two fairly weakly-reflecting interfaces. Therefore this phenomenon can be adequately described in the simplest approximation of two-beam interference. Note that for an interference pattern to exist, the temporal coherence length should be at least of the order of twice the distance between the interfaces. In our case, based on the known gain-profile width in a semiconductor, $\Delta\nu \sim 400 \text{ cm}^{-1}$, we come to a coherence length of order $25 \mu\text{m}$, which means that this condition cannot be met in principle.

¹Line 3 reads "dealt with in preceding interim report. Since it is the subthreshold ..."

Nevertheless, semiconductor lasers clearly exhibit the presence of interference. It is a consequence of two factors:

- (i) the emitting atoms reside between the resonator mirrors characterized by large reflection coefficients;
- (ii) the medium has the property of ~~enhancing substantially~~ the gain.

To use the language of quantum mechanics, the presence of the mirrors increases the probability of emission along the resonator axis, the wavelength of this radiation meeting satisfactorily the resonance condition. Viewed from the standpoint of classical optics, this means that the resonant wavelength produces constructive interference on the resonator axis and, hence, the highest intensity of emitted light (for equal emitted power per atom). This is the reason for the spatial dependence of the amplified-radiation spectrum and for its on-axis monochromatization. This pattern of the phenomenon suggests that it should be observed only in the near-axial region, where each atom of the medium produces a series of images in the mirrors making up a linear periodic emitting structure. The linearity of this structure breaks down as one moves away from the axis, and this is what is responsible for the destruction of the constructive interference. It should be pointed out that the significance of the equivalent sources in this series falls off with increasing number of the mirror reflections involved the faster, the smaller is the reflection coefficient. It may be suggested that as the gain increases and approaches the lasing threshold, the effective length of this emitter series should increase, so that interference should be observed within a progressively more narrow axial region; also, since the spectral selectivity of this emitter set increases in the axial direction, the spectral lines should become narrower. These considerations can apparently be used as a basis for development of a more comprehensive theory of the observed pattern.

2. Computer Program for the Calculation of Lasing Onset in Lasers with Unstable Resonators

Our computer program draws upon the unique mathematical model of the process, which was developed by us earlier and based on an analysis of

the spatial evolution and amplification of the luminescence emitted at each point of the excited active medium in all directions. The spatial evolution is calculated within the geometrical-optics approximation (for unstable resonators with a magnification coefficient $M \geq 2$ this approximation is known to guarantee a satisfactory accuracy). To cut down computer time, the medium parameters and the values of total radiation density over the resonator cross sectional area were assumed to be the same as on the axis; our experience in computing the characteristics of lasers with telescopic resonators shows the errors due to this assumption to be insignificant. Although this model was constructed for lasers with short inversion times, for which it is particularly useful, its universality and usefulness cannot be questioned.

Let us present the main relations needed here. In the case of a cylindrical active medium with diameter $2a$ and length L equal to the resonator mirror separation, we can write for the radiation density

$$\rho(z, t) = \frac{1}{4c} \int_{z-ct}^{z+ct} \ln \left[1 + \frac{r_0^2(z')}{B_{zz}^2} \right] \gamma \left(z', t - \frac{|z-z'|}{c} \right) \times \\ \times \exp \left\{ \int_{z'}^z k_g \left(z'', t - \frac{|z-z''|}{c} \right) dz'' \right\} dz'.$$

Here z is the coordinate along the resonator axis (with the origin at the concave mirror), t is the time reckoned from the pump turn-on (and, hence, from the appearance of spontaneous radiation on lasing frequency), γ is the volume density of spontaneous radiation power, B_{zz} is the ray matrix element of the optical system representing a section of the resonator-equivalent optical line between the cross sections lying at the coordinates z' and z , r_0 is one half of the zone diameter on the z' plane, which is seen from the observation point at z and was calculated by means of this matrix with due account of beam obstructions, and k_g is the gain coefficient.

This equation, for whose derivation the reader can be referred to [1], should be solved together with the equations describing the change in the state of the medium acted upon by the pumping and by the radiation field

with density ρ initiating stimulated emission. The state of the medium, in its turn, governs the quantities γ and k_g .

This system of integrodifferential equations yields the power W of the output radiation and its angular distribution:

$$W(t) = c\pi\sigma^2 \left(1 - \frac{1}{M^2}\right) \int_{L-ct}^L F(z', L, t) dz',$$

$$\Phi(\varphi, t) = \int_{L-ct}^L F(z', L, t) \eta(z', \varphi) dz' \cdot \left[\int_{L-ct}^L F(z', L, t) dz' \right]^{-1},$$

where $\Phi(\varphi, t)$ is the fraction of radiation power confined to a far-field solid angle φ ,

$$\eta(z', \varphi) = \begin{cases} q^2, & q \leq 1 \\ 1, & q \geq 1 \end{cases}, \quad q = \frac{\varphi B_{\pi}}{2r_0(z') + 2\sigma|D_{\pi}|},$$

B_{π} and D_{π} are elements of above-mentioned matrix for $z = L$.

In our earlier work, we developed the corresponding computational program. It was written in the presently-obsolete programming language designed for the BESM-6 computers in use at the time. While in order to cut down computer time, it was subjected to some simplifications in addition to those mentioned above, it was found to be fully adequate in the interpretation of experimental data obtained on copper-vapor lasers [1] and excimer lasers [2], as well as when designing lasers of these types.

Work performed within this Grant has included writing computer programs in Fortran and Pascal, which are much better in all respects. Our calculations, in particular, use exact, rather than length-averaged, values of γ and k_g , the resonator length is divided into 40 sections, and not 10, as before, and so on.

The program consists of several modules corresponding to individual elements of the system and different stages of the solution. This permits us to modify it at will for use with different resonator parameters, pumping techniques, and kinetic models of the medium.


Data are inputted by straightforward file editing by means of a special editor built into the program and started whenever required. Output files receive output data; a subprogram for viewing graphs on the monitor is naturally also provided.

These programs are presently in the stage of check-out using the familiar copper-vapor laser model. In the next stage, the check-out will be completed, and the various modifications of the programs to deal with the geometry characteristic of semiconductor lasers will be developed, after which the programs will be submitted to Philips Lab.

The problems associated with the possible role of a number of effects whose inclusion would make the programs too bulky even for present-day computers pose severe difficulties. It still remains unclear how small is the value of M at which the crossover from geometrical-optics to diffraction approximation becomes necessary; what is the role of radiation coherence effects in the onset of lasing; to what extent the presence of a low- Q resonator affects the spatial distribution of noise radiation, and so on. Some of these problems may be resolved in the stage of comparison of calculations with experimental data.

REFERENCES

1. Ananiev Yu.A. and Anikichev S.G. , "Problem of kinetics of unstable resonator lasers with short-time inversion population". - Journal of Technical Physics, 1983, v. 53, N 10, p. 1959
2. Ananiev Yu.A., Anikichev S.G. *et al*, "Kinetics of oscillations of excimer laser with telescopic unstable resonator and polarization radiation output". - Journal of Technical Physics, 1989, v. 59, N 7, p. 1100

Principal Investigator: 

4.

CONSIDERATIONS ABOUT SUMMARY
"ASE PATTERNS & MODE FORMATION IN
UNSTABLE RESONATORS" (OF G.DENTE *et al*)
AND INFORMATION ABOUT PROCEEDING PROGRESS IN CREATION OF
PROGRAM OF LASING ONSET
(INTERIM REPORT)

2

1. Comments upon report "ASE patterns & mode formation in
unstable resonators" (of G.Dente *et al*)

A. Preliminary remarks

- a) Despite of general appreciation to Siegman, one can not say that he invented the unstable resonator. Really, unstable resonators were well known much earlier than publication of Siegman's paper (of 1965); he formulated only supposition that in spite of common opinion the unstable resonator can turn be useful.
- b) Results of calculation in geometrical approximation coincide with corresponding formula in the book "Laser Resonators and the Beam Divergence Problem" of Anan'ev (p. 144, line 18 from top) after replacing $L \rightarrow 2L$ and $R = -R_m$.
- c) General view of experimental ASE patterns (Spatio-Spectral Patterns) is in accordance with considerations provided in our first report. Indeed, much below threshold (current of 180 ma or 220 ma) we see phenomena of classical optics, near threshold and over it the pictures correspond to principal resonator mode.

B. About regenerative amplifier properties of unstable resonators

This section is very interesting, but reading is aggravated because of too short text. For example, senso of "t" is not explained; one does not point out whether near field or far field is provided on all figures, and so on.

Method of Neumann series is fully appropriate to analyzing the problem. We notice only that more obvious deduction of formula

2 line A a) 2 reads "invented the unstable resonator. Really unstable resonators were well ..."

$F(x) = [1 + K + K^2 + \dots] S(x)$ is the substitution instead of F in the right part of expression $F(x) = S(x) + K \cdot F$ the same right part of the same expression, then subsequent analogous substitution, and so on.

It is not clear why the summary comprises a consideration of case of plane resonator; it is not clear too why on the last line of p.12 we have sign \approx rather than $=$.

The numerical results are useful and clear, but some qualitative laws was published before in small-known (for Western) papers of Russian scientists.

Namely, it was shown in [1, 2] that converging wave of unstable resonator possesses maximum gain; relevant evaluation was made in the same works. Subsequent discussion on this theme was published in [3-5].

The answer to the question on beginning of p. 13 is provided for arbitrary resonators in works of Berenberg ([6-8] and others). He solved by standard variation method namely the same problem which is formulated on p.14 of Summary.

Finally we notice that it was shown in some paper [9, 10] that all attempts to pass converging wave through unstable resonator lied to dramatic increase in value of output angular divergence. It can be explained in such manner. If we want to achieve a high energy transformation efficiency, our amplifier have to work in regime of deep saturation. In this regime value of gain on several last passes through resonator is no high, and fluxes of energy on this steps of converging wave evolution are nearly equal. At the same time the converging wave has the diffraction value of divergence only on sole last step; on other steps it has smaller area of cross section and therefore the bigger divergence.

2. INFORMATION ABOUT PROCEEDING PROGRESS IN CREATION OF PROGRAM OF LASING ONSET

We have created a program for calculation of laser onset in the case when an active medium takes up only a part of resonator length. This one will be provided in our final report. At present we are informing about some results of calculations having been done by this program.

All figures relate to the following equations and values of laser parameters:

$$\frac{\partial N_1}{\partial t} = \frac{N_1 - N_3}{\tau_n} - \frac{\rho}{h\nu}(N_3 - N_1) - \frac{N_3}{\tau}, \quad \frac{\partial N_2}{\partial t} = \frac{\rho}{h\nu}(N_3 - N_2) + \frac{N_3}{\tau},$$

$$N_1 + N_2 + N_3 = N = \text{const}, \quad \frac{1}{\tau_n} = \frac{1}{T_1} \left[1 - \exp\left(-\frac{t}{T_2}\right) \right].$$

$$\text{Light density } \rho(z, t) = \int_{-a}^{+a} F(z', z, t) dz',$$

$$F(z', z, t) = \frac{1}{4c} \frac{r_0^2(z')}{B_w^2} \gamma\left(z', t - \frac{|z - z'|}{c}\right) \cdot \exp\left\{ \int_{z'}^z k\left(z', t - \frac{|z - z'|}{c}\right) dz' \right\},$$

$$\text{output power } W(t) = cna^2 \left(1 - \frac{1}{M^2}\right) \int_{-a}^{+a} F(z', z, t) dz',$$

$$\text{gain coefficient } k = \sigma(N_3 - N_2),$$

$$\text{power of spontaneous radiation source } \nu = h\nu N_3 / \tau;$$

at last, active zone radius $a = 0.5$ cm, active zone length 40 cm,

$N = 2.5 \cdot 10^{14} \text{ cm}^{-3}$ (in the some cases $2 \cdot 10^{13} \text{ cm}^{-3}$), $\sigma = 10^{-14} \text{ cm}^2$,

active medium temperature 1600°C (its value effects on initial level population with bearing in mind the statistical weight 1, 6 and 4 for level

1, 2, 3 respectively), $\tau = 770 \cdot 10^{-9} \text{ s}$, $T_2 = 10^{-8} \text{ s}$, $\lambda = 0.51 \mu$, resonator

magnification coefficient $M = 30$, resonator length from 40 to 60 cm.

On fig. 1 are provided curves for cases of two different programs of calculation — with averaging gain coefficient over the active medium length and without it. One can easily see that difference exists but is not too large.

Fig. 2 and fig. 3 correspond to cases of $N = 2.5 \cdot 10^{14} \text{ cm}^{-3}$ and $N = 2 \cdot 10^{13} \text{ cm}^{-3}$ respectively. One can see the increase in atom density leads to dramatic increase in depth of time modulation. Fig. 4 and 5 manifest the existence of the same law in the case when active medium fills only the part of resonator length.

Fig. 6 belongs to case of intermediate resonator length; finally, on fig. 7 is represented temporal spectrum of laser pulsa in one out of regimes.

References

1. Anan'ev *et al*, JETP v. 58, pp.786—793, 1970
2. Anan'ev, Quantum Electronics (J. of USSR), 1971, N 6, pp. 3—34
3. Zemskov *et al*, Quantum Electronics (J. of USSR), v. 1, p. 863, 1974
4. Isaev *et al*, Quantum Electronics (J. of USSR), v. 1, p. 1379, 1974
5. Anan'ev, Quantum Electronics (J. of USSR), v. 2, pp. 1138—1141
6. Balashov *et al*, Quantum Electronics (J. of USSR), v. 2, pp. 281—286, 1975
7. Balashov *et al*, Optika i spektroskopiya v. 44, pp. 312—319, 1978
8. Balashov *et al*, Optika i spektroskopiya v. 44, pp. 1131—1135
9. Anan'ev *et al*, Quantum Electronics (J. of USSR), v. 2, pp. 1952—1956, 1975
10. Anan'ev *et al*, Quantum Electronics (J. of USSR), v. 6, pp. 1773—1775, 1979

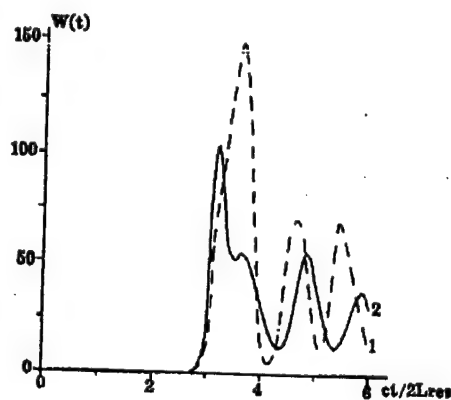


Figure 1. Laser pulse calculated with averaging over the active medium length (2) and without it (1).

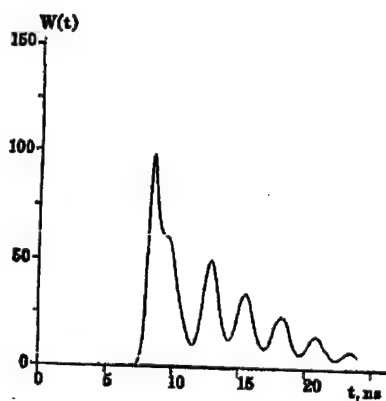


Figure 2. Laser power as a function of time for $L_{res} = 40$ cm.

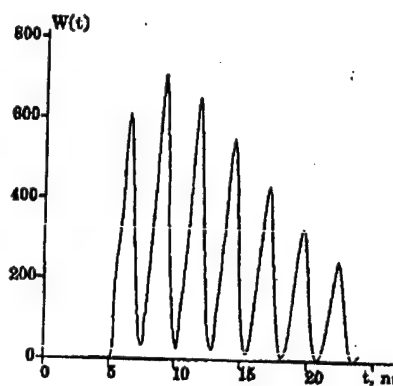


Figure 3. Laser power as a function of time for $L_{res} = 40$ cm, $N = 2 \times 10^{15} \text{ cm}^{-3}$

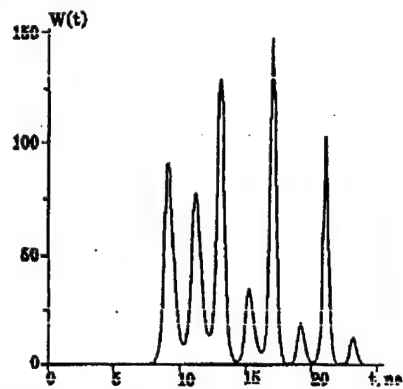


Figure 4. Laser power as a function of time for $L_{res}=60$ cm

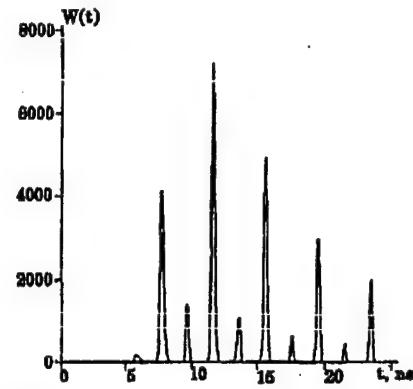


Figure 5. Laser power as a function of time for $L_{res}=60$ cm, $N=2 \times 10^{15} \text{ cm}^{-3}$

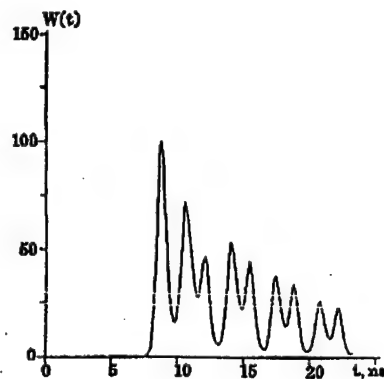


Figure 6. Laser power as a function of time for $L_{res}=50$ cm

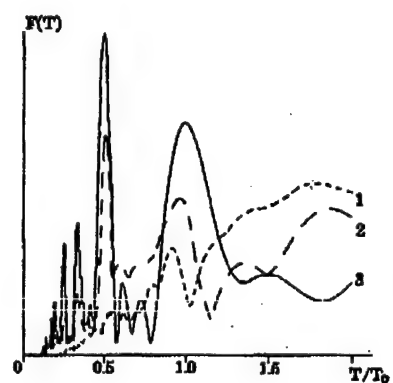


Figure 7. Temporal spectrum of laser pulse: 1 - $L_{res}=40$ cm, 2 - $L_{res}=50$ cm, 3 - $L_{res}=60$ cm.

PROGRAM OF CALCULATION FOR KINETICS OF LASERS WITH TELESCOPIC RESONATORS

1. INP.EXE IS A FILE FOR INITIATION OF THE PROGRAM

```

PROGRAM INP;
{$M 4000,2000,10000}
USES CRT, DOS;
CONST
  RP = ' ';
VAR
  M,L,A,WL,SIGMA,N,TAU,T1,T2,DT,TF: SINGLE;
  NV,NP,NZ: INTEGER;
  F: TEXT;
  VARFLG: BOOLEAN;
BEGIN
  CLRSCR;
  WRITELN('      PROGRAM OF CALCULATION FOR KINETICS OF LASERS');
  WRITELN('      WITH TELESCOPIC RESONATORS ');
  WRITELN(' Press any key');
  READKEY;
  {$I-}
  ASSIGN(F, INP1.DAT);
  RESET(F);
  IF IORESULT <> 0 THEN BEGIN
    WRITELN(RP, 'FILE "INP1.DAT" NOT FOUND. ');
    READLN;
    HALT
  END;
  {$I+}
  READLN(F, M);
  READLN(F, L);
  READLN(F, A);
  READLN(F, WL);
  CLOSE(F);
  CLRSCR;
  WRITELN(RP, ' PARAMETERS OF CAVITY : ');
  WRITELN(RP, ' RESONATOR MAGNIFICATION      M =', M:3:1);
  WRITELN(RP, ' RESONATOR LENGTH          L(CM) =', L:3:1);
  WRITELN(RP, ' TUBE RADIUS              A(CM) =', A:3:1);
  WRITELN(RP, ' RADIATION WAVELENGTH (MICRO) =', WL:1:3);
  WRITELN(RP, ' DO YOU WANT TO CHANGE DATA (YES,N-NO)? ');
  WRITELN;
  WHILE NOT KEYPRESSED DO
  CASE READKEY OF
    'Y', 'y', CHR(13): BEGIN
      SWAPVECTORS;
      EXEC('ED.EXE', INP1.DAT);
      SWAPVECTORS;
      IF DOSERROR <> 0 THEN BEGIN
        WRITELN(RP, 'UNABLE TO EDIT FILE');
        READLN;
        HALT(1)
      END;
    END;
  END;
  CLRSCR;
  {$I-}
  ASSIGN(F, INP2.DAT);
  RESET(F);
  IF IORESULT <> 0 THEN BEGIN
    WRITELN(RP, 'FILE "INP2.DAT" NOT FOUND. ');

```

```

READLN;
HALT
END;
{S1+1}
READLN(F, SIGMA);
READLN(F, N);
READLN(F, TAU);
CLOSE(F);
CLRSCR;
WRITELN(RP, ' PARAMETERS OF MEDIUM:');
WRITELN(RP,
' STIMULATED EMISSION CROSS SECTION (1.E-14*CM2) = ', SIGMA :4:2);
WRITELN(RP,
' MEDIUM DENSITY (1.E14/CM3) = ', N :4:2);
WRITELN(RP,
' UPPER LEVEL LIFETIME (NS) = ', TAU :4:2);
WRITELN(RP, ' DO YOU WANT TO CHANGE DATA (Y-YES,N-NO)? ');
WRITELN;
WHILE NOT KEYPRESSED DO:
CASE READKEY OF
'Y', 'y', CHR(13): BEGIN
SWAPVECTORS;
EXEC('ED.EXE', 'INP2.DAT');
SWAPVECTORS;
IF DOSERROR <> 0 THEN BEGIN
WRITELN(RP, 'UNABLE TO EDIT FILE');
READLN;
HALT(1)
END
END;
END;
END;
WRITELN(RP, ' FOLLOWING PUMPING ( 1/TH) VARIANTS ARE SUGGESTED :');
WRITELN(RP, ' 1 - 1/TH=1/T1*(1-EXP(-T/T2)) (T AND TH IN NS)');
WRITELN(RP, ' 2 - 1/TH=1/T1 ');
WRITELN(RP, 'INPUT NUMBER OF VARIANT');
READLN(NV);
IF NV=1 THEN BEGIN
WRITELN(RP, ' T1 = ? NS');
READ(T1);
WRITELN(RP, ' T2 = ? NS');
READ(T2);
ASSIGN(F, 'NAK.DAT');
RESET(F);
REWRITE(F);
WRITELN(F, NV);
WRITELN(F, T1:4:4);
WRITELN(F, T2:4:4);
CLOSE(F);
END;
IF NV=2 THEN BEGIN
WRITELN(RP, ' T1 = ?');
READ(T1);
ASSIGN(F, 'NAK.DAT');
RESET(F);
REWRITE(F);
WRITELN(F, NV);
WRITELN(F, T1:4:4);
CLOSE(F);
END;
DT:=L/15;
WRITELN(' TIME OF DOUBLE CAVITY PASS =',DT:2:3,' NS');
WRITELN(' INPUT OPERATING PARAMETERS OF THE PROGRAM');
WRITELN(' NUMBER OF STEPS ON THE CAVITY LENGTH (NL<=40)');

```

```

READLN(NZ);
NP:=ROUND(400/2/NZ);
WRITELN(RP, ' NUMBER OF DOUBLE CAVITY PASS ');
WRITELN(' NP<=' ,NP:3);
READ(NP);
ASSIGN(F, 'N.DAT');
RESET(F);
REWRITE(F);
WRITELN(F, NZ);
WRITELN(F, NP);
CLOSE(F);
SWAPVECTORS;
EXEC('TELESC.EXE,');
SWAPVECTORS;
END.

```

2. INPUT PARAMETERS ARE LOCATED IN FILES *.DAT: INP1,INP2,N,NAK

FILE INP1.DAT:

```

30.0 - RESONATOR MAGNIFICATION
40.0 - RESONATOR LENGTH (CM)
1.0 - TUBE RADIUS (CM)
0.51 - RADIATION WAVELENGTH (MICRONS)

```

FILE INP2.DAT:

```

1.0 - STIMULATED EMISSION CROSS SECTION (1.E-14*CM2)
2.5 - MEDIUM DENSITY (1.E14/CM3)
770. - UPPER LEVEL LIFETIME (NS)

```

FILE N.DAT

```

40 - NUMBER OF STEPS ON CAVITY LENGTH
5 - NUMBER OF DOUBLE CAVITY PASS

```

FILE NAK.DAT

```

1 - NUMBER OF PUMPING VARIANT
10. - PUMPING RATE IN NS
10. - PUMPING INCREASE RATE IN NS

```

3. RESULTS

FILE W(T).DAT

OUTPUT RADIATION POWER AS A FUNCTION OF TIME

```

1 COLUMN - TIME IN NS
2 COLUMN - TIME IN UNITS OF DOUBLE CAVITY PASS TIME
3 COLUMN - OUTPUT POWER (KW)

```

FILE PHI(T).DAT

OUTPUT POWER FRACTION WITHIN THE DIFFRACTION ANGLE AS A FUNCTION OF TIME:

```

1 COLUMN - TIME IN NS
2 COLUMN - TIME IN UNITS OF DOUBLE CAVITY PASS TIME
3 COLUMN - OUTPUT POWER FRACTION WITHIN THE DIFFRACTION ANGLE

```

FILE W_PHI.DAT

CONTAINS CURRENT VALUES OF OUTPUT ENERGY (mJ) IN A PULSE AND ITS FRACTION WITHIN THE DIFFRACTION ANGLE:

```

1 COLUMN - TIME IN NS
2 COLUMN - PULSE ENERGY IN mJ
3 COLUMN - PULSE ENERGY FRACTION WITHIN THE DIFFRACTION ANGLE

```

```

      REAL FUNCTION VN(NV,T1,T2,T)
C SUBROUTINE OF PUMPING RATE CALCULATION
      VN=0.
      IF(NV.EQ.2) VN=1./T1
      IF(NV.EQ.1) VN=1./T1*(1.-EXP(-T/T2))
      RETURN
      END
      REAL FUNCTION R0(IZ)
C SUBROUTINE OF CALCULATION FOR AN EFFECTIVE MEDIUM RADIUS IN A
C POINT Z
      REAL M,L
      COMMON /RESON/ A,L,M,NZ,DZ,DT
      Z0=(ABS(IZ)/2./NZ)-INT(ABS(IZ)/2./NZ)
      R0=A
      IF(Z0.GT..5.AND.Z0.LT.1.) R0=A/M*(2.-M+2*(M-1.)*Z0)
      RETURN
      END
      REAL FUNCTION DETB(IZ0,IZ,N)
C SUBROUTINE FOR CALCULATION OF A BEAM MATRIX ELEMENT B FOR
C TRANSITION FROM Z TO Z0
      REAL M,L
      COMMON /RESON/ A,L,M,NZ,DZ,DT
      IF(IZ0.EQ.IZ) GOTO 1
      LJ=1
      IF(IZ.LT.IZ0) LJ=2
      GOTO ((1,2),LJ)
1      DETB=0.
      N=0
      RETURN
C 0=<Z0<=L Z=Z2>Z0
11      F=IZ/2./NZ
      N=INT(F-.00001)
      T=0.
      IF((N*ALOG(M)).LT.(10.*ALOG(10.))) T=1./(M**(2*N))
      IF(N.EQ.0) T=1.
      IF(T.GT.N.AND.F.LE.(N+.5)) DETB=DZ*(NZ-IZ0+(IZ-2.*N*NZ)*T+NZ/(M
P -1.)*(1.-M*T))
      IF(F.GT.(N+.5).AND.F.LE.(N+1.)) DETB=DZ*(IZ-2.*N*NZ-IZ0+(M-1.)/N
P Z*(NZ-IZ0)*(IZ-(2.*N+1.)*NZ)+NZ/(M-1.)*(1.-T))
      RETURN
      END
C 0=<Z0<=L Z=Z1<Z0
21      F=-IZ/2./NZ
      N=INT(F+.49999)
      T=0.
      IF((N*ALOG(M)).LT.(10.*ALOG(10.))) T=1./(M**(2*N))
      IF(N.EQ.0) T=1.
      IF(F.GT.(N-.5).AND.F.LE.N) DETB=DZ*(IZ0*T-(IZ+(2.*N-1.)*NZ)+NZ/(
P M-1.)*(1.-T*M))
      IF(F.GT.N.AND.F.LE.(N+.5)) DETB=DZ*(NZ/(M-1.)*M*(1.-T)+T*(IZ0-(I
P Z+2.*N*NZ)+(M-1.)/M*IZ0*(IZ+2.*N*NZ)/NZ))
      RETURN
      END
      REAL FUNCTION DETD(IZ0,IZ,N)
C SUBROUTINE FOR CALCULATION OF A BEAM MATRIX ELEMENT D FOR
C TRANSITION FROM Z TO Z0
      REAL M,L
      COMMON /RESON/ A,L,M,NZ,DZ,DT
      IF(IZ0.EQ.IZ) GOTO 1
      J=1
      IF(IZ.LT.IZ0) J=2
      GOTO ((1,2),J)
1      DETD=1.
      N=0

```

```

CONTINUE
END DO
IF(W.NE.0.) WPI=WPI/W
IF(W.EQ.0.) WPI=0.
DO JZ=IT,1
IZ1=NZ+JZ
RO1=RO1+DETF(NZ,IZ1,IT)*DZ
END DO
RO=RO1
IF(W.LT.0.) W=0.
IF(WPLT.0.) WPI=0.
WRITE(1,*)IT*DT,IT/2./NZ,W
WRITE(2,*)IT*DT,IT/2./NZ,WPI
SW=SW+W*DT*1.E-3
SP=SP+WPI*W*DT*1.E-3
IF(SW.NE.0.) WRITE(3,*)IT*DT,SW,SP/SW
RETURN
END
REAL FUNCTION DETF(IZ,IZ1,IT)
C SUBROUTINE FOR CALCULATION OF RADIATION FLOW FROM A LAYER DZ
C IN A POINT Z1 TO A POINT Z
REAL M,L
COMMON /RESON/ A,L,M,NZ,DZ,DT
COMMON /MEDIA/ PHI0,SIGMA,G0,C0,TAU,SW,SP
COMMON /EV1/ Y1(0:40,0:400)
COMMON /EV2/ Y2(0:40,0:400)
BB=ALOG(ABS(DETB(IZ,IZ1,N)))
DD=N*ALOG(M)
G=GAIN(IZ,IZ1,IT)
RR=ALOG(RO(IZ1))
I=IT-ABS(IZ-IZ1)
IF(LLT.0) I=0
F=(ABS(IZ1)/2./NZ)-INT(ABS(IZ1)/2./NZ)
IF(F.GE.0.AND.F.LE.5) J=INT(F*2*NZ)
IF(F.GE.5.AND.F.LE.1.) J=INT(2*NZ*(1.-F))
GAMMA=Y2(J,I)
GG=ALOG(TAU)
DEIF=GAMMA*EXP(G-GG-2.*(DD-RR+BB))/4./30.
RETURN
END
REAL FUNCTION GAIN(IZ,IZ1,IT)
C SUBROUTINE FOR CALCULATION OF RADIATION GAIN AT PASS FROM A POINT
C Z1 TO A POINT Z
REAL M,L
COMMON /RESON/ A,L,M,NZ,DZ,DT
COMMON /MEDIA/ PHI0,SIGMA,G0,C0,TAU,SW,SP
COMMON /EV1/ Y1(0:40,0:400)
COMMON /EV2/ Y2(0:40,0:400) IP=IT-ABS(IZ-IZ1)
IF(IP.LT.0) IP=0
S=0.
IQ=1
IF(IZ1.GT.IZ) IQ=-1
IZ2=IZ1
DO I=IP,IT-1
F=(ABS(IZ2)/2./NZ)-INT(ABS(IZ2)/2./NZ)
IF(F.GE.0.AND.F.LE.5) J=INT(F*2*NZ)
IF(F.GE.5.AND.F.LE.1.) J=INT(2*NZ*(1.-F)) S=S+Y2(J,I)-Y1(J,I)
IZ2=IZ2+IQ
END DO
GAIN=S*DZ*SIGMA
IF(IZEQ.IZ1) GAIN=0.
RETURN
END

```

```

      NN=INT(200/NZ)
      IF(NP.GT.NN) NP=NN
      WRITE(*,*) 'STEP IS CHANGED'
      WRITE(*,*) 'N=',NZ
      IF(NZ.LE.40) GOTO 999
998   CLOSE(1)
      CLOSE(2)
      CLOSE(3)
      STOP
77    IF(INT(IT/NZ/2)*2*NZ.EQ.IT) WRITE(*,*) 'NP=',INT(IT/2/NZ)
      END DO
      CLOSE(1)
      CLOSE(2)
      CLOSE(3)
      END
      REAL FUNCTION RO(IZ,IT)
C SUBROUTINE OF CALCULATION FOR OUTPUT POWER AND SATURATING
C INTENSITY IN A POINT (Z,T)
      REAL M,L
      COMMON /RESON/ A,L,M,NZ,DZ,DT
      COMMON /MEDIA/ PHI0,SIGMA,G0,C0,TAU,SW,SP
      COMMON /EV1/ Y1(0:40,0:400)
      COMMON /EV2/ Y2(0:40,0:400)
      RO1=Y2(IZ,IT)/30./TAU
      IF(IZEQ.0) GOTO 1
      IF(IZEQ.NZ) GOTO 2
      DO JZ=-IT,IT
      IZ1=IZ+JZ
      IF(JZ.NE.0) RO1=RO1+DETF(IZ,IZ1,IT)*DZ
      END DO
      RO=RO1
      RETURN
1     DO JZ=-IT,IT
      IZ1=JZ
      IF(JZ.NE.0) RO1=RO1+DETF(0,IZ1,IT)*DZ
      END DO
      RO=RO1
      RETURN
2     W=RO1*3.14159*A*A*(1.-1./M/M)/2.*G0
      WPI=0.
      DO JZ=-IT,-1
      IZ1=NZ+JZ
      CC=DETF(NZ,IZ1,IT)*DZ
      RO1=RO1+CC
      W=W+CC*(1.-1./M/M)*3.14159*A*A*G0
      D=ABS(DETD(NZ,IZ1,N))
      B=ABS(DETB(NZ,IZ1,N))
      IF (B.EQ.0.) GOTO 12
      IF (D.EQ.0.) GOTO 11
      QF=0.
      IF((N*A.LOG(M)).LT.(8.*A.LOG(10.))) QF=1./(M**N)
      Q2=2.*R0(IZ1)*QF+2.*A*ABS(D)
      Q1=PHI0*B
      Q=1.
      IF(ABS(Q1).LT.ABS(Q2)) Q=ABS((Q1/Q2)**2)
      WPI=WPI+CC*Q*(1.-1./M/M)*3.14159*A*A*G0
      GOTO 12
11    Q1=N*A.LOG(M)+A.LOG(PHI0*B)
      Q2=A.LOG(2.*R0(IZ1))
      Q=0.
      IF(Q1.GE.Q2) Q=1.
      IF(Q.NE.1.) Q=EXP(Q1-Q2)
      WPI=WPI+CC*Q*(1.-1./M/M)*Q*3.14159*A*A*G0

```

VARIANT OF THE PROGRAM TEDESC.FOR TAKES INTO ACCOUNT A DISTRIBUTION OF
INVERSION OVER THE CAVITY LENGTH

```

PROGRAM TEDESC
CHARACTER*44 ANSWER
REAL M,L
COMMON /RESON/ A,L,M,NZ,DZ,DT
COMMON /MEDIA/ PHI0,SIGMA,G0,C0,TAU,SW,SP
COMMON /EV1/ Y1(0:40,0:400)
COMMON /EV2/ Y2(0:40,0:400)
1  FORMAT(F8.1,A44)
   OPEN(UNIT=1,FILE='INP1.DAT')
   READ(1,1)M,ANSWER
   READ(1,1)L,ANSWER
   READ(1,1)A,ANSWER
   READ(1,1)WL,ANSWER
   CLOSE(1)
   OPEN(UNIT=1,FILE='INP2.DAT')
   READ(1,1)SIGMA,ANSWER
   READ(1,1)C0,ANSWER
   READ(1,1)TAU,ANSWER
   CLOSE(1)
   OPEN(UNIT=1,FILE='NAK.DAT')
   READ(1,*)NV
   READ(1,*)T1
   T2=0.
   IF(NV.EQ.1) READ(1,*)T2
   CLOSE(1)
   OPEN(UNIT=1,FILE='N.DAT')
   READ(1,*)NZ
   READ(1,*)NP
   CLOSE(1)
   SIGMA=SIGMA*C0
   PHI0=1.2E-4*WL/A
   G0=6.626176*90./WL*C0
999 DO IX=0,NZ
     Y1(IX,0)=0.
     Y2(IX,0)=0.
     END DO
     DZ=L/NZ
     DT=DZ/30.
     OPEN(UNIT=1,FILE='W(T).DAT')
     OPEN(UNIT=2,FILE='PHI(T).DAT')
     OPEN(UNIT=3,FILE='W_PHI.DAT')
     SW=0.
     SP=0.
     DO IT=1,NT
       T0=(IT-1)*DT
       IS=IT-1
       IND=0
       DO IX=0,NZ
         X1=1.-Y1(IX,IS)-Y2(IX,IS)
         IF(X1.LT.0.) X1=0.
         IF(Y1(IX,IS).LT.0..OR.Y1(IX,IS).GT.1.) Y1(IX,IS)=0.
         IF(Y2(IX,IS).LT.0..OR.Y2(IX,IS).GT.1.) Y2(IX,IS)=0.
         DER1=30.*SIGMA*RO(IX,IS)*(Y2(IX,IS)-Y1(IX,IS))+Y2(IX,IS)/TAU
         DER2=(X1-Y2(IX,IS))*VN(NV,T1,T2,T0)-DER1
         Y1(IX,IT)=Y1(IX,IS)+DER1*DT
         Y2(IX,IT)=Y2(IX,IS)+DER2*DT
         IF((ABS(Y1(IX,IT))+ABS(Y2(IX,IT))),GT.1.) IND=1
       END DO
       IF(IND.EQ.0) GOTO 77 IF(SW.GT.1.) GOTO 999
       NZ=NZ+10

```

```

      RETURN
C 0<=Z0=<L Z=Z2>Z0
11 F=IZ/2./NZ
   N=INT(F-.00001)
   IF(F.GT.N.AND.F.LE.(N+.5)) DETD=1.
   IF(F.GT.(N+.5).AND.F.LE.(N+1.)) DETD=1.+(M-1.)/NZ*(IZ-(2.*N+1.)*
P NZ)
      RETURN
C 0<=Z0<=L Z=Z1<Z0
21 F=-IZ/2./NZ
   N=INT(F+.49999)
   T=0.
   IF((N*ALOG(M)).LT.(10.*ALOG(10.))) T=1./(M**(2*N))
   IF(N.EQ.0) T=1.
   IF(F.GT.(N-.5).AND.F.LE.N) DETD=T
   IF(F.GT.N.AND.F.LE.(N+.5)) DETD=T*(1.+(M-1.)/M*(IZ+2.*N*NZ)/NZ)
      RETURN
      END

```


5. CONCLUSIONS

The initial report by Anan'ev was the 'geometric' view. This view holds that the unstable resonator has a ray that has the required integer number of waves in round trip at locations outside the optical axis. The path is longer, so the frequency shift is down (to longer wavelengths). The rays are not normal to the surface of the mirrors, but some feedback is expected due to diffraction of the small spot. Al Paxton⁶ at PL/LIDA had espoused such a view. The preferred ray is one that splits the angle equally at each side of the resonator and has the required frequency to give integer waves of optical path in a round trip. The spontaneous emission meeting this criterion will be retained in the resonator and amplified to much higher intensity than that which does not meet this criterion.

The problem with the geometrical view is that it does not require coherence between the two sides of the resonator. A 'modal' approach, proposed by Greg Dente³, assumes that the modes are coherent with respect to themselves on the opposite sides of the resonator. This view holds that the whole mode can be fed by spontaneous emission all over the resonator into its adjoint mode (converging wave). The propagation of the beam, which keeps clear fringe patterns as it goes from near-field to far-field, suggests that the modal view is superior. Both views are compatible since the modal view predicts hot spots exactly where the geometric view finds its resonant rays. The difference is that the geometric view holds the two spots uncorrelated, where the modal view holds them to consist of two modes, one in phase and one out of phase. Spontaneous emission and gain at the core of the resonator should make the in-phase mode dominant. Professor Anan'ev's March 1995 report presents a multiple pass geometric viewpoint that bridges the modal and geometric views.

An interesting variation of the modal view comes from comparing the

⁶ Private communication

situation to ordinary dielectric waveguides. This is most appropriate for the situation where the divergence in the resonator is produced continuously by a transverse index of refraction variation or an imbedded lens train, rather than by curved reflectors at the ends of the resonator. The difference is that the modes are evanescent in the core of the resonator and radiate in the outer regions. This is just the opposite of the situation in ordinary dielectric waveguide modes.

The significance of these points occurs when the laser is switched from below threshold to above threshold operation. The existence of a mode inside the cavity might effect the speed of the turn on, and a structured pattern might seed filaments in a diode laser medium. The sum of all the frequencies is, however, fairly smooth, so the gain saturation due to the sum of the modes does not itself produce filamentation. The laser modes that do turn on as the gain is increased lie at the central axis of the herringbone pattern. These modes grow to fill the lateral extent of the resonator, replacing the light in the below threshold spontaneous emission driven modes. Spontaneous emission that does not fall into the preferred frequencies is quickly rejected by the resonator. Thus the existence of these patterns does not significantly affect the performance of a laser above threshold. Their utility may be as a diagnostic tool to evaluate the quality of the processing used to manufacture these lasers.

ASE Patterns & Mode Formation **in Unstable Resonators**

Greg Dente - GCD

Mike Tilton - RPS

Chuck Moeller - PL

Outline

I. Introduction & Overview

- Geometric motivation for converging and diverging modes

II. ASE Data -- Spatio-Spectral Patterns

- Experimental method & representative data

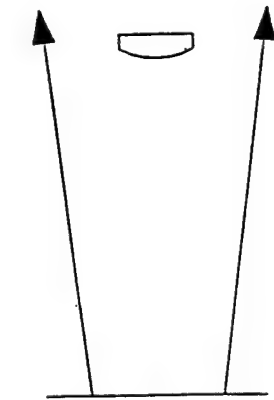
III. Regenerative Amplifier Properties of Unstable Resonators

- Overview of the method
- Optimum Inputs -- "converging waves"
- Converging waves & ASE Patterns $g < g_{\text{TH}} \rightarrow g \sim g_{\text{TH}}$
- Gain vs. ν and Petermann - K factor

IV. Conclusions ???

Unstable Resonators

- Invented by A. Siegman in 1965 -----

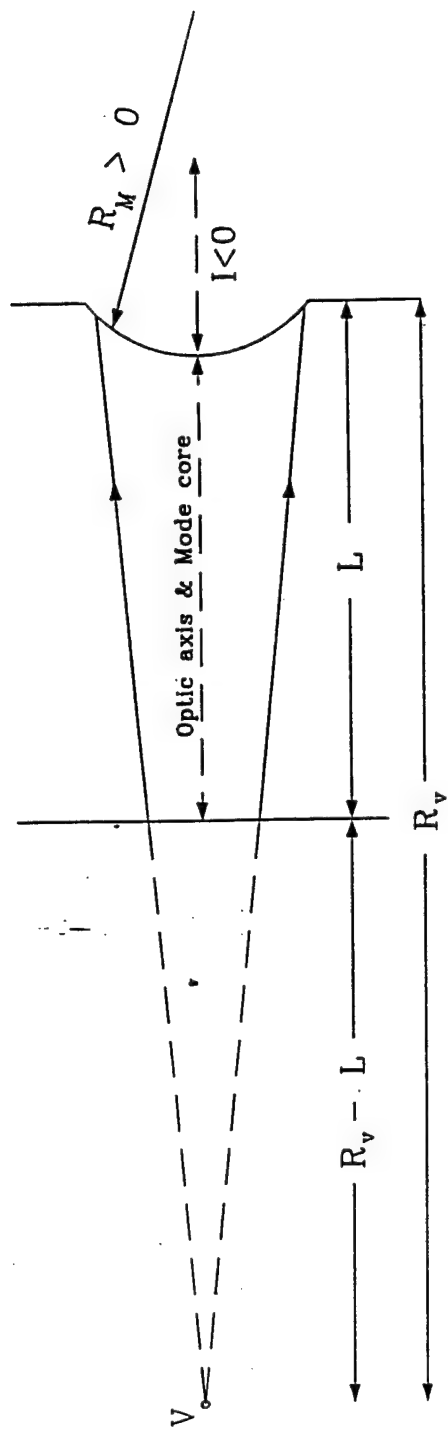


- Large Mode Volumes
- Near diffraction limited performance (good mode discrimination)
- Insensitive to misalignments and aberrations in the medium

• Applications to Semiconductor Lasers

- Bogatov, et. al. (1980) - polished facet mirror
- Craig, PhD Dissertation (1985) - etched facet mirrors
- Yariv, Salzman, et. al. (1985-'87) - etched facet mirrors
- OGI, PL, UNM, et. al. (1989-present) - ion milled, etched, lens train

I. Basic Design Idea – Geometric Modes



- V = virtual mode source. Mode appears to radiate from V after each round-trip:
- Reflect off of Front Facet: $\frac{1}{I} + \frac{1}{R_v} = \frac{-2}{R_M} \quad I < 0 \text{ (virtual)}$
- Reflect off of Back Facet: Image I through the back facet and require that it sit on top of $V \rightarrow (R_v - L = |I| + L) \quad I = -R_v + 2L$

Constant virtual mode source (mode bright spot)

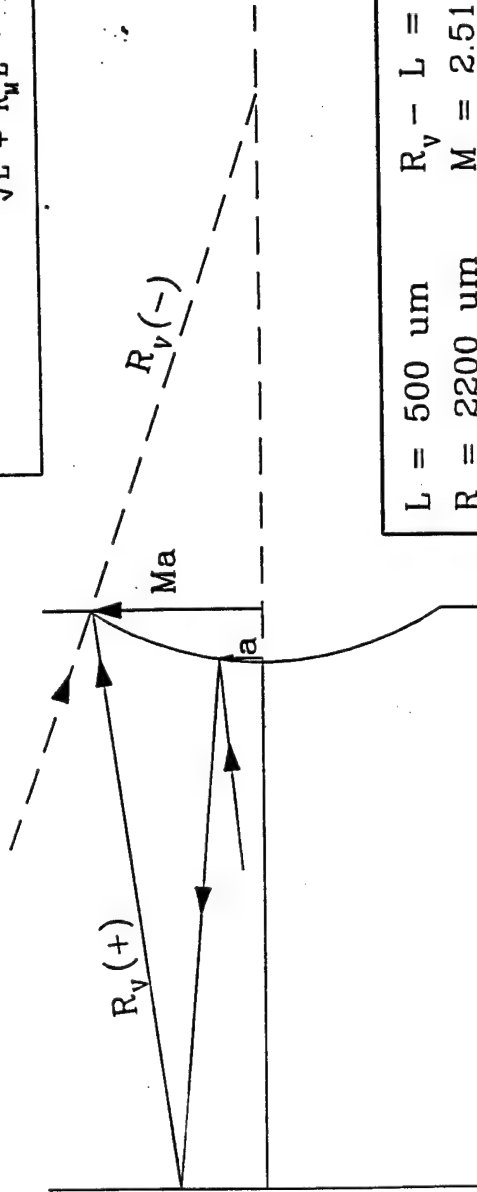
$$\frac{1}{2L - R_v} + \frac{1}{R_v} = \frac{-2}{R_M}$$

$$R_v(R_v - 2L) = R_M L$$

Solve for R_v for given R_M and L

$$R_v - L = \pm \sqrt{L^2 + R_M L}$$

$$M = \frac{R_v}{R_v - 2L} = \frac{\sqrt{L^2 + R_M L} + L}{\sqrt{L^2 + R_M L} - L}$$



$$\begin{array}{ll} L = 500 \text{ um} & R_v - L = \pm 1162 \text{ um} \\ R_M = 2200 \text{ um} & M = 2.51 \end{array}$$

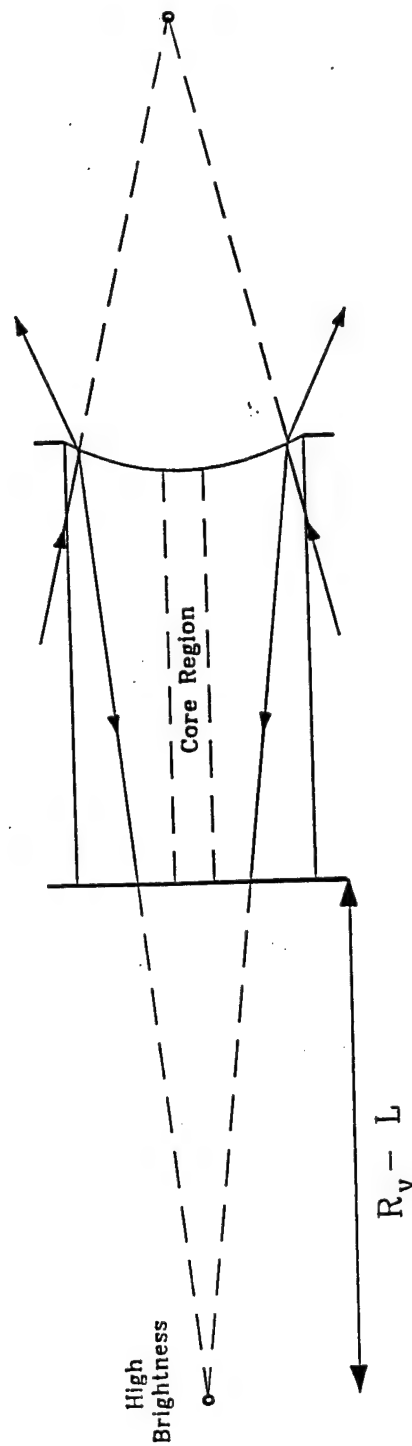
Summary

$$\text{Mode virtual source} = R_v - L = \pm \sqrt{L^2 + R_M L}$$

$$\text{Mode magnification} = \dot{M} = \frac{\sqrt{L^2 + R_M L} + L}{\sqrt{L^2 + R_M L} - L}$$

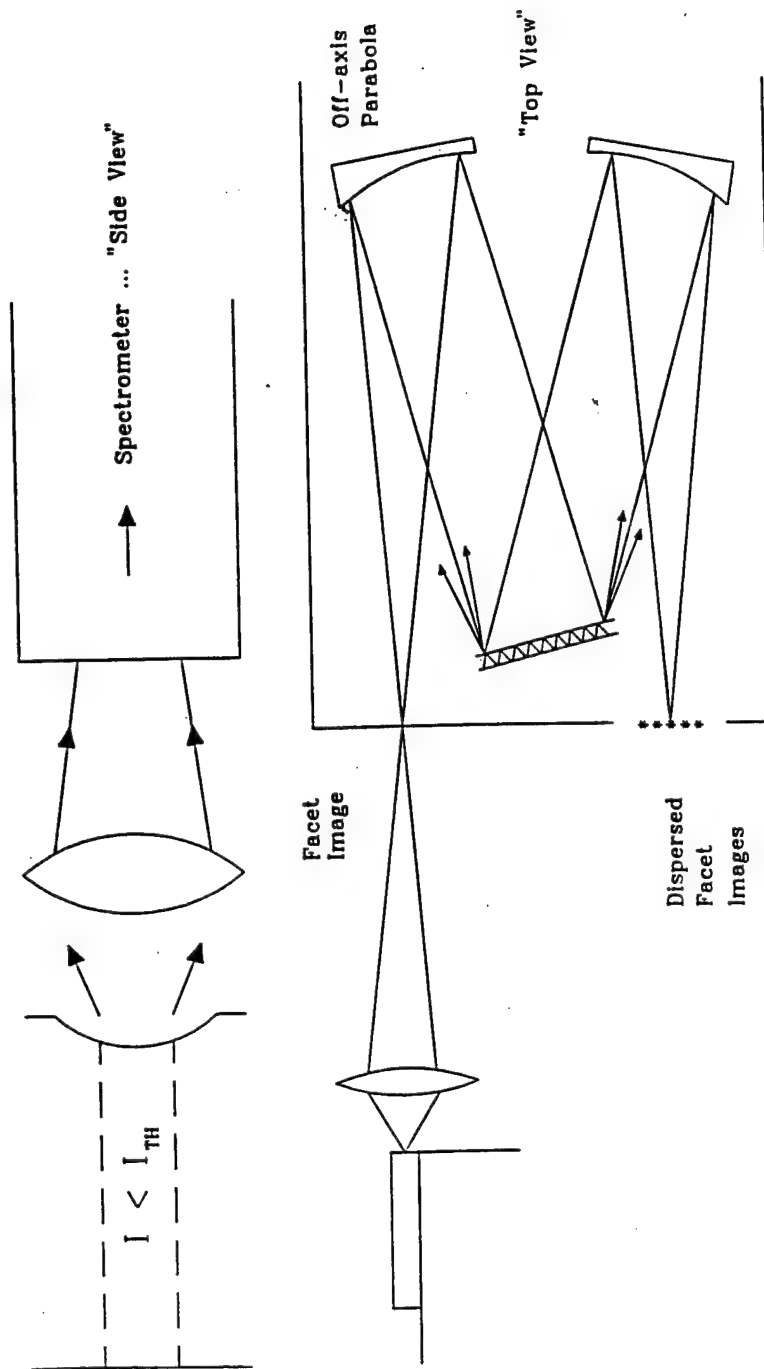
(rate of expansion)

UR has a narrow core region (the MO) feeding
off-axis angled amplifier regions



II. ASE Patterns -- Spatio-Spectral Patterns

Over the last few months, OGI and PL have begun analyzing the ASE radiating from unstable resonators:



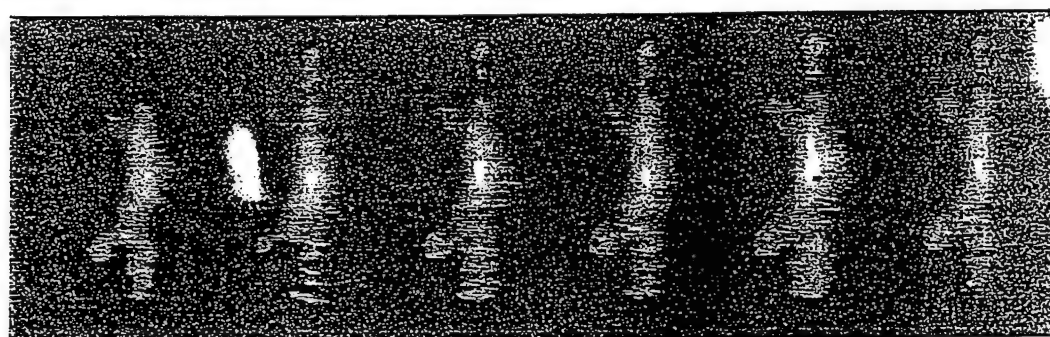
Spectral Pattern

InGaAs/AlGaAs CW URSL 200 X 500 μm

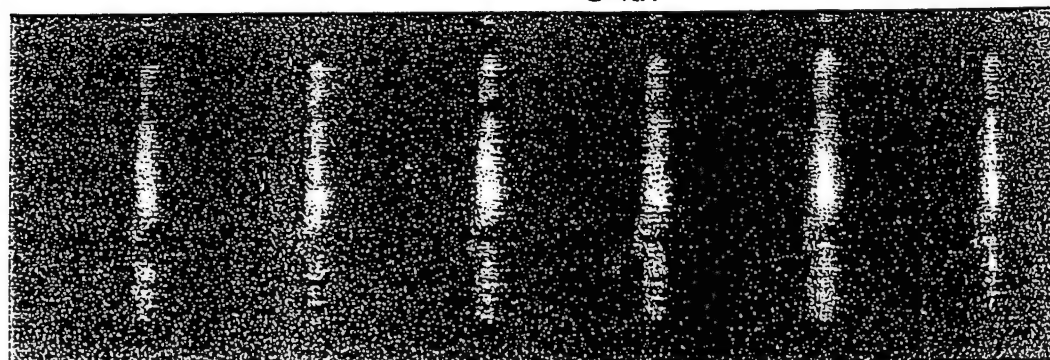
@ 0.75 X Ith



9670 \AA @ 0.9 X Ith



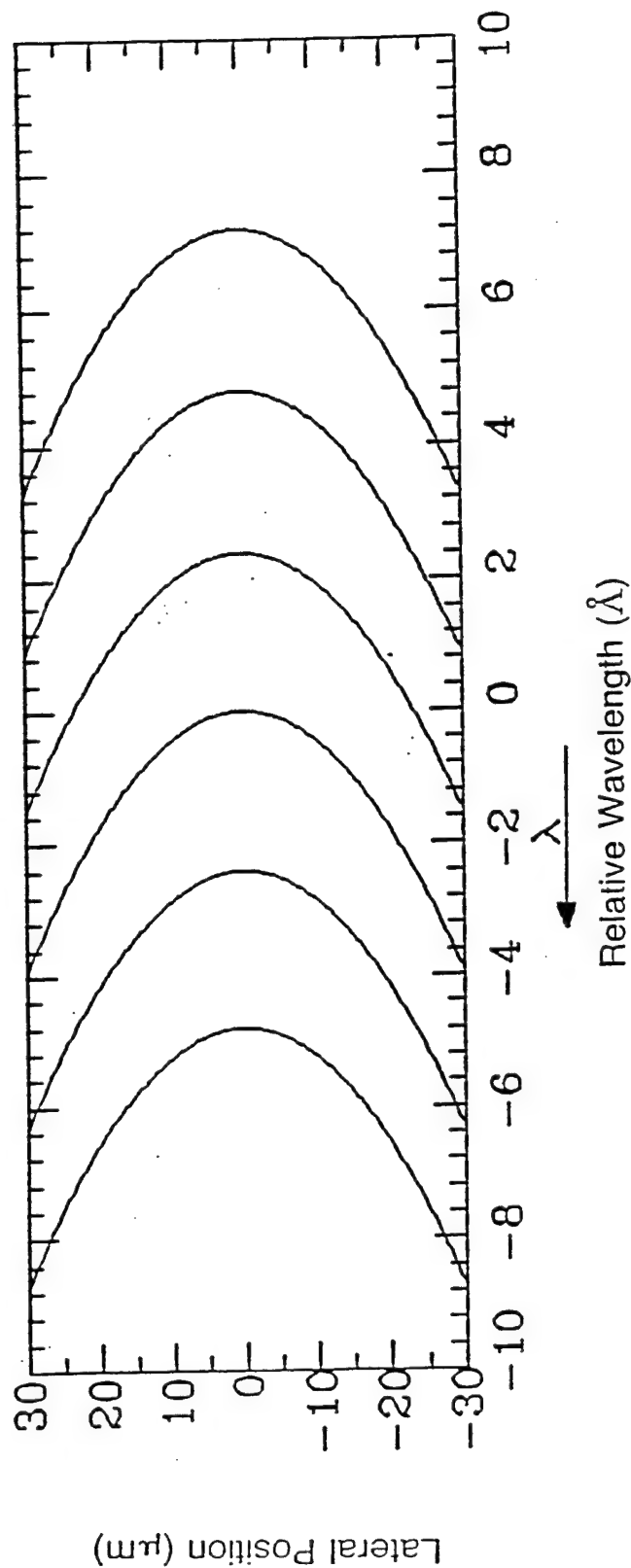
@ Ith



Ref. Z Bao, et al,

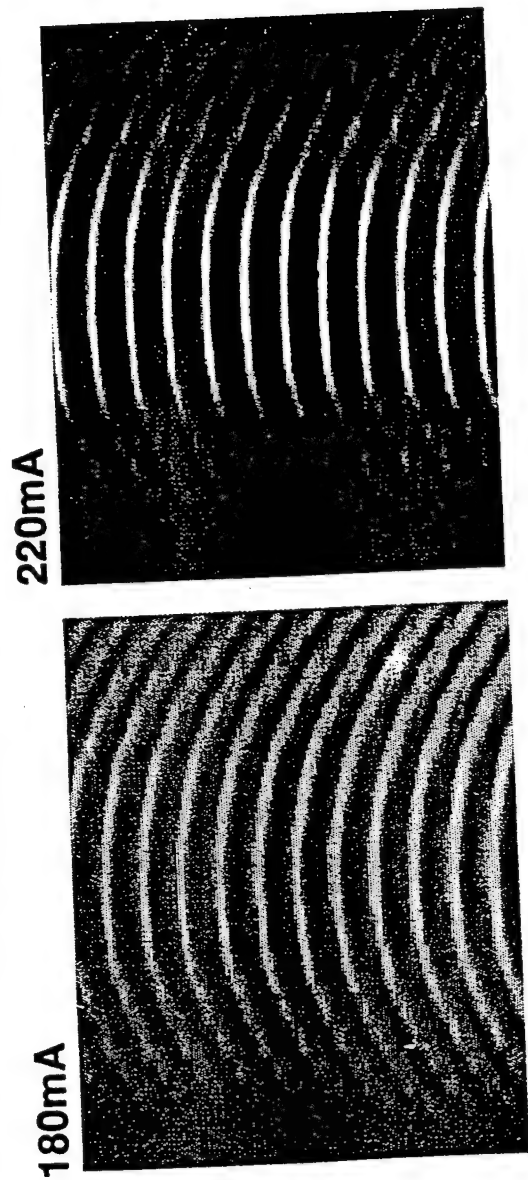
Spatio-Spectral Characteristics of a High Brightness CW InGaAs/AlGaAs Unstable Resonator Semiconductor Laser. Elec. Letters, Vol. 29,(18) Sept. 1993

500 μm Long URSL, Mag=2.5, Mode Spacing=2.4 Angstrom

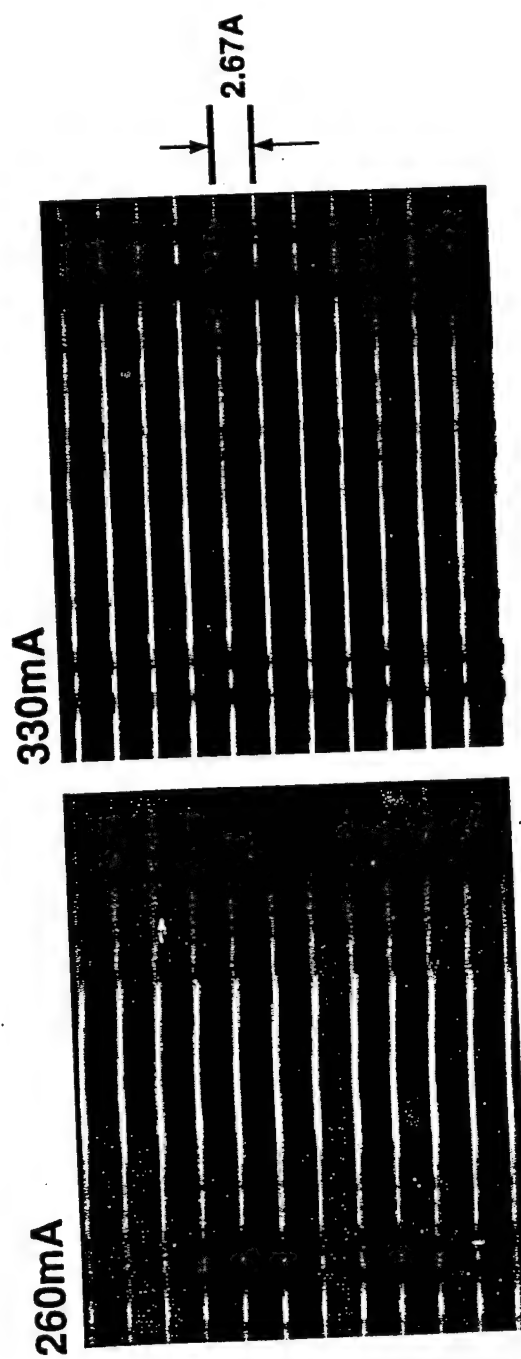


Spatio-spectral pattern of a cold cavity unstable resonator ($200 \times 500 \mu\text{m}$)

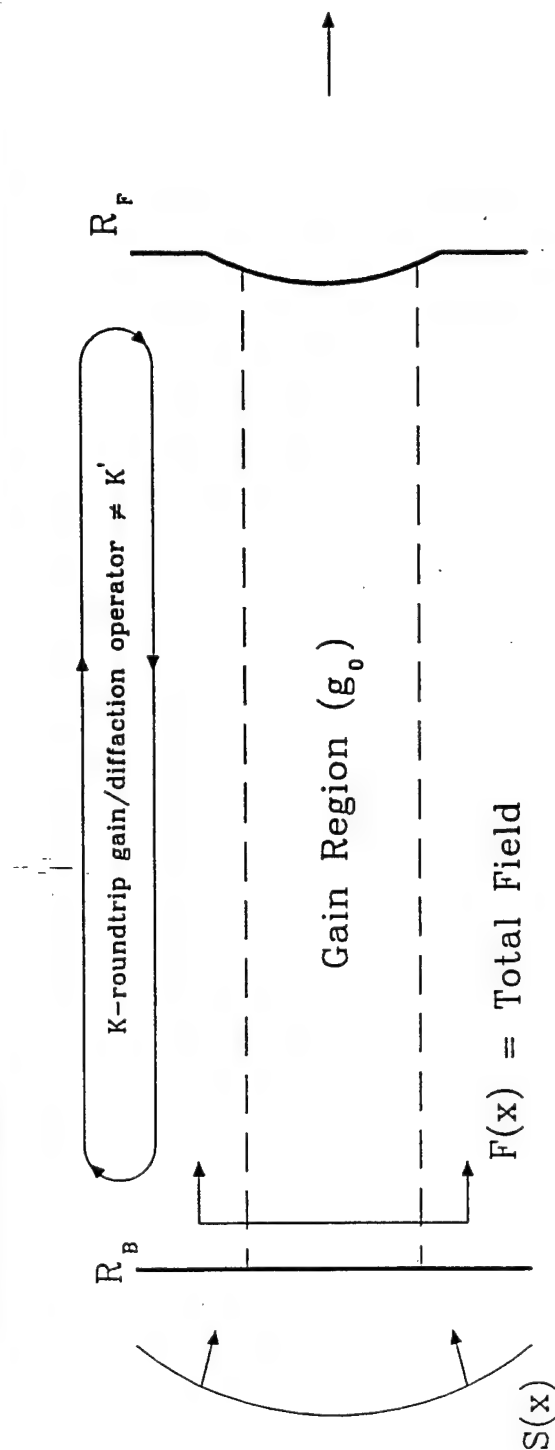
HALF SYMMETRIC UR : R=2200um L=500um



Nominal threshold = 300mA



III. Regenerative Amplifier Properties of Unstable Resonators



If we define the circulating field at the entry facet as $C(x)$:

$$F(x) = t \cdot S(x) + C(x) \quad \text{also, } C(x) = \int K(x, x') F(x') dx' = K * F$$

Integral equation for regenerative ASE patterns.

$$F(x) = K * F + t \cdot S(x)$$

Neumann series solution method:

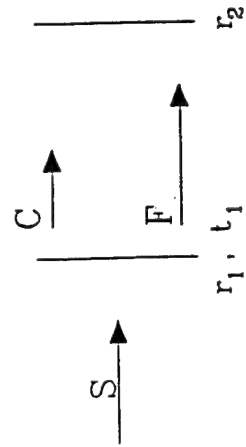
$$[I - K] * F = t S(x)$$

$$F(x) = [I - K]^{-1} * t S(x) = \underbrace{\{I + K* + K* K* + K* K* K* + \dots\}}_{\text{Neumann Series = Regenerative Gain}} t S(x)$$

Neumann Series = Regenerative Gain

◦ Series can converge for $\|K\| < 1$. Solve for F for a given S(x).

Ex. Planar Fabry-Perot

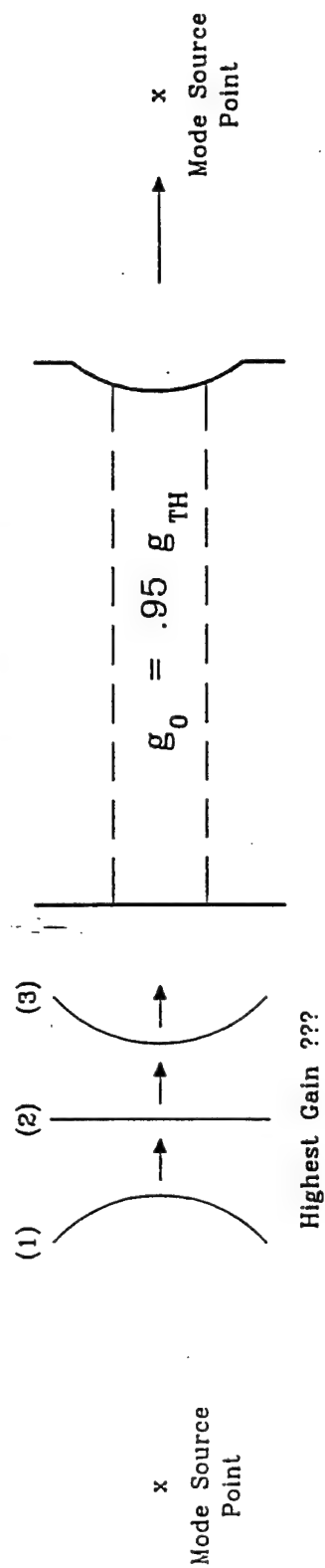


$$F = C + t S \quad \text{and} \quad C = r_1 r_2 e^{2i\vartheta} F$$

$$F(1 - r_1 r_2 e^{2i\vartheta}) = t S \quad \rightarrow \quad F = \frac{t S}{1 - r_1 r_2 e^{2i\vartheta}}$$

$$\approx [1 + (r_1 r_2 e^{2i\vartheta}) + (r_1 r_2 e^{2i\vartheta})^2 + \dots] t S$$

Optimum Inputs --- . What form for $S(x)$ gives maximum gain
 at a given frequency ? $F = (1 - K)^{-1} \cdot tS$



(1) Diverging Wave

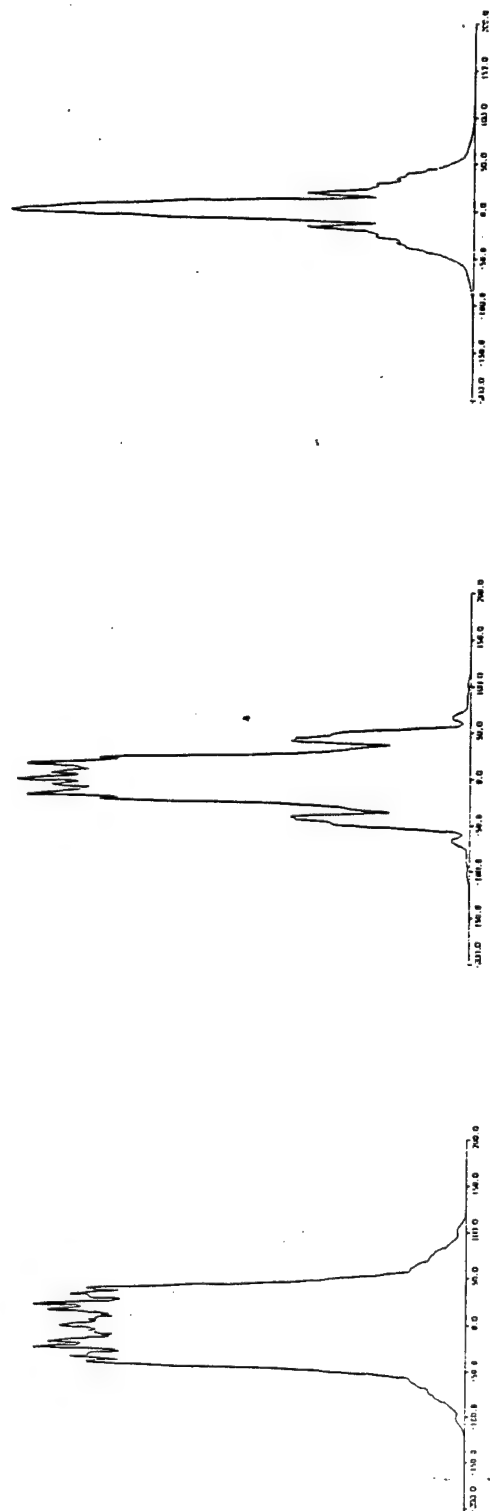
Gain = 6.91

(2) Plane Wave

Gain = 8.68

(3) Converging Wave

Gain = 102.01



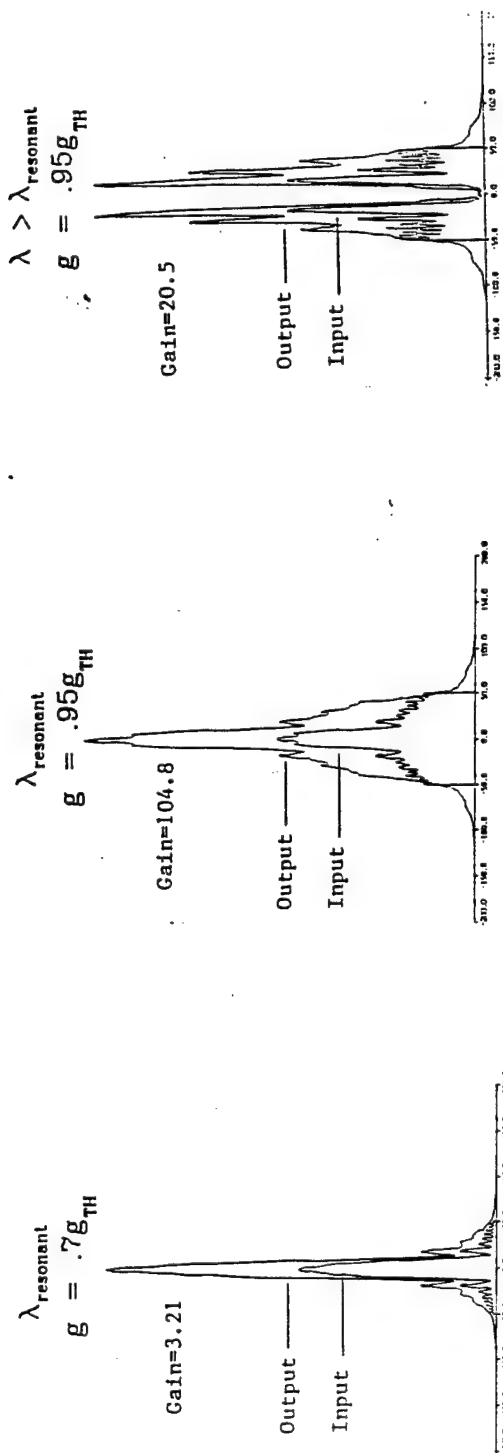
Integral Equation for S:

$$a S = T S \quad T = T^\dagger \quad \text{Hermitian}$$

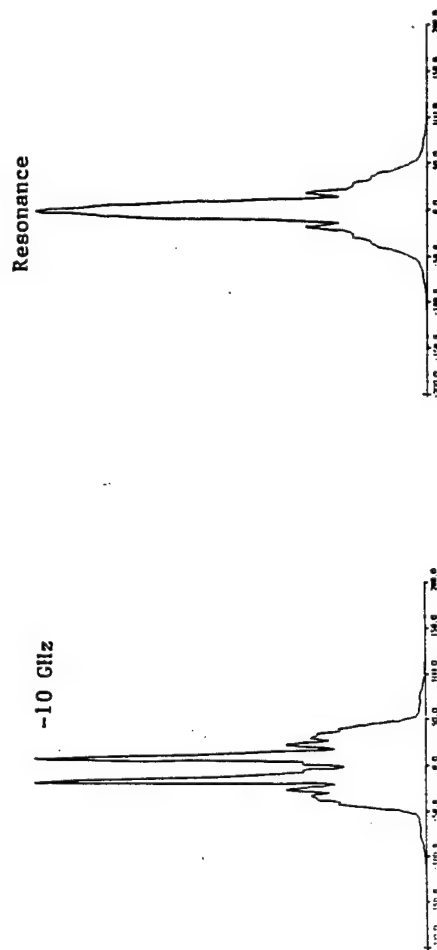
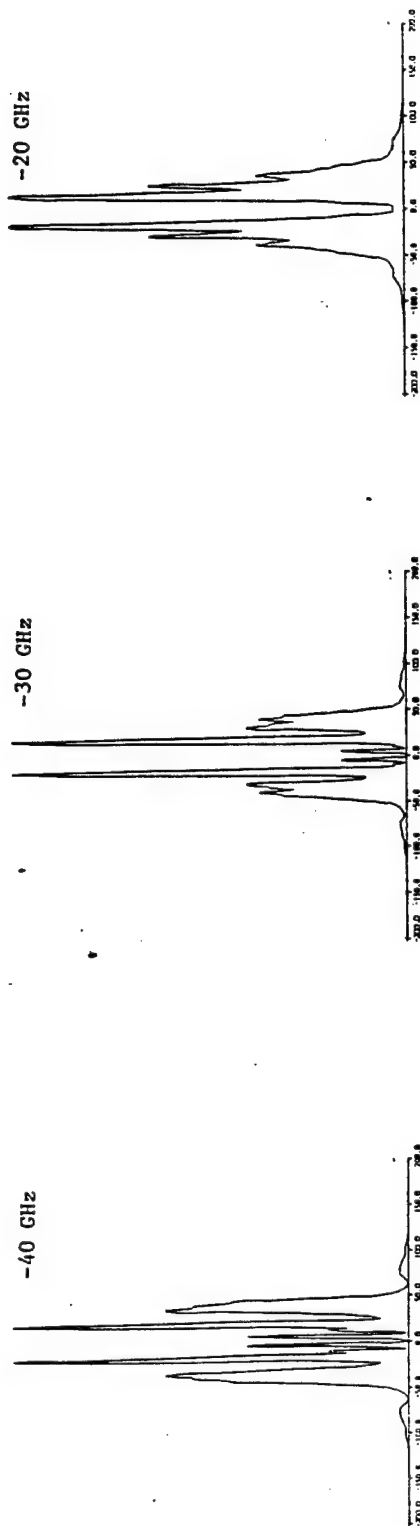
$$= \frac{1}{1 - K^\dagger} \frac{1}{1 - K} S, \quad K \sim \text{depends on } g \text{ and } \lambda$$

Below threshold this is equivalent to $a^{-1} S = (1 - K) (1 - K^\dagger) S$.

Solutions are readily obtained numerically:



Fixed gain with λ varying

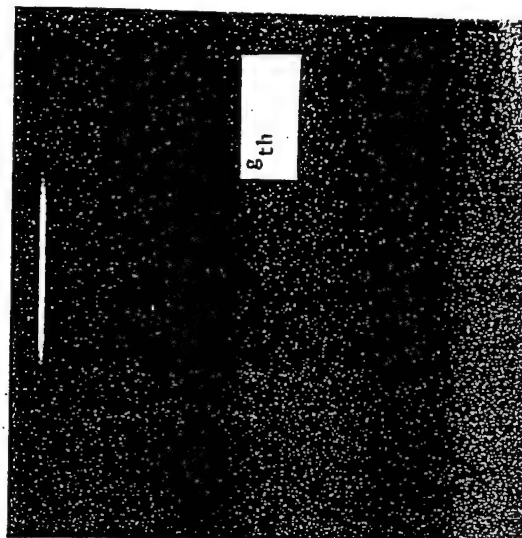
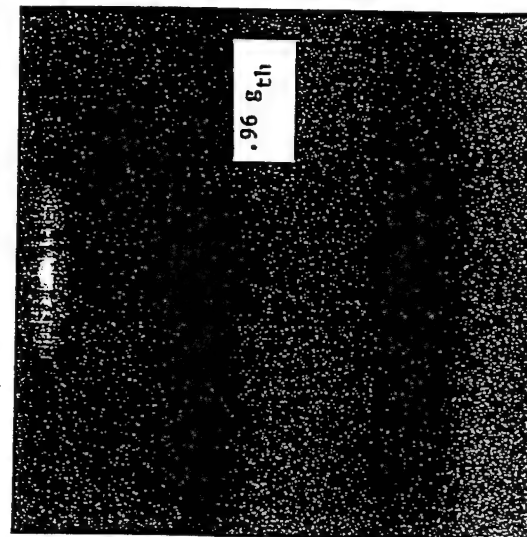
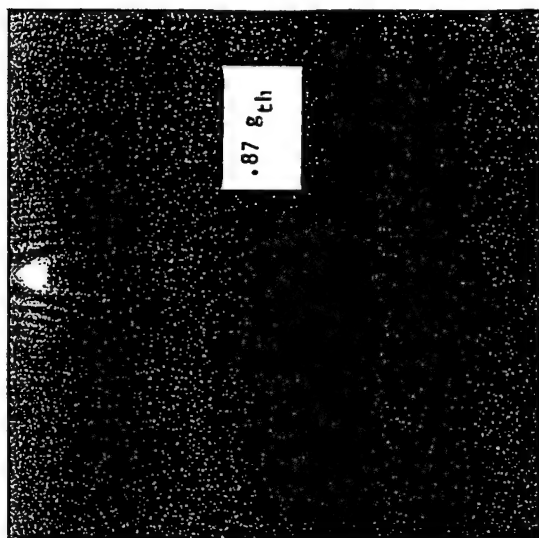
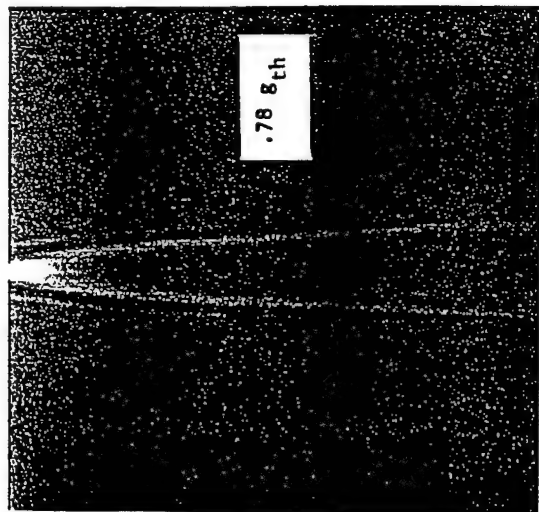


ASE Patterns



- If we concentrate on the optimum input waves, how is the ASE distributed ?

Grey Scale Combinations



Useful Function Sets

K_{ω} = roundtrip propagator for an unstable resonator $K_{\omega} \neq K_{\omega}^{\dagger}$

$$\left[\begin{array}{l} \text{Modes: } K_{\omega} U_n = \lambda_n U_n \\ \text{Adjoint Modes: } K_{\omega}^{\dagger} V_n = \bar{\lambda}_n V_n \end{array} \right] \quad \lambda_n = \bar{\lambda}_n \text{ and } \int dx V_m U_n = \delta_{mn}$$

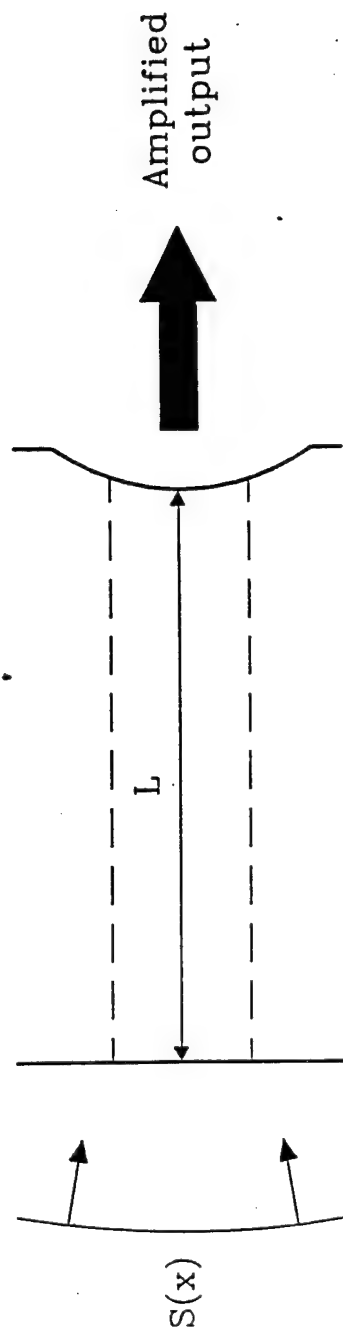
$\{U_n\}$ and $\{V_n\}$ are biorthogonal

$$a S_{\omega} = \underbrace{\frac{1}{1 - K_{\omega}^{\dagger}} \frac{1}{1 - K_{\omega}}}_{\text{Hermitian}} S_{\omega}$$

and $\{S_n\}$ are orthogonal

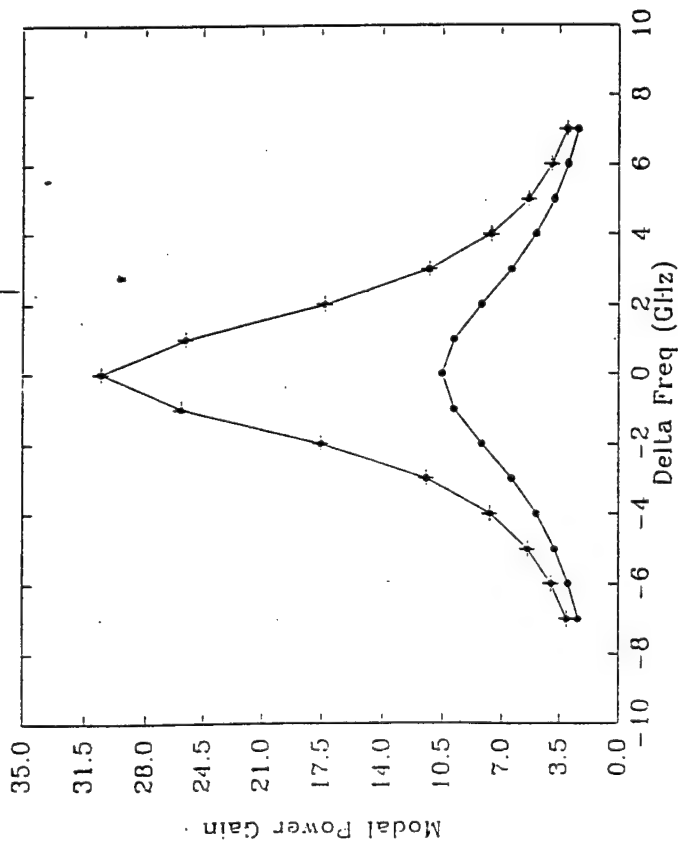
In Hermitian systems: $K_{\omega} = K_{\omega}^{\dagger}$ and $\{U_n\} = \{V_n^*\} = \{S_n\}$.

Gain versus ν and Petermann K



- Vary the input frequency $\nu(\lambda)$ -- What happens ?
 - Maximize gain at $L = \text{integer} * \frac{\lambda}{2}$ "standing wave on axis"
 - Gain decreases rapidly as λ varies about $\bar{\lambda}$

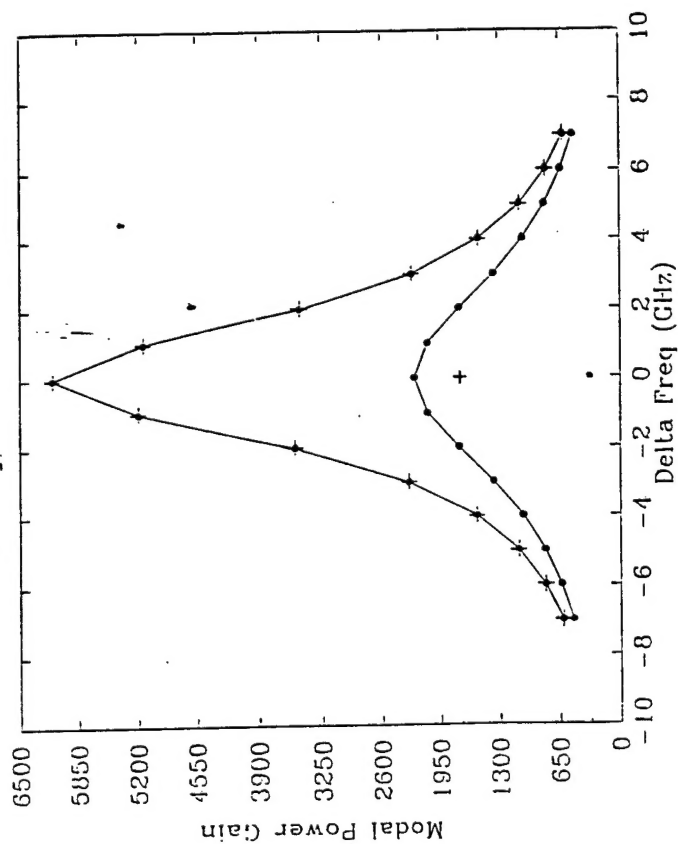
1st case: $S = U_o$ (diverging mode input) & Power gain on mode $U_o = G$



$$\text{Gain} = \frac{\left| \int V_o F dx \right|^2}{\int |U_o|^2 dx} = \frac{\text{Total Power Out}}{\text{Power In}}$$

$$G_{\text{peak}} (\Delta \nu)^2 = (\Delta \nu_{\text{cc}})^2$$

2nd case: S = optimum (converging wave) input
Power gain on mode $U_o = G$



$$\overline{\text{Gain}} = \frac{\left| \int V_o F dx \right|^2}{\text{Power In}} > \frac{\text{Total Power Out}}{\text{Power In}}$$

$$\overline{G}_{\text{peak}} (\Delta \nu)^2 = K (\Delta \nu_{cc})^2 \quad K = \text{Petermann} - K$$

$$\overline{G}_{\text{peak}} = K G_{\text{peak}}$$

Petermann - K and Laser Linewidth

With an optimum converging wave input, the power gain on the dominant mode satisfies the relation:

$$\bar{G}_{\text{peak}} (\Delta\nu)^2 = K G_{\text{peak}} (\Delta\nu)^2 = K (\Delta\nu_{\text{cc}})^2$$

Schawlow - Townes Linewidth Derivation -

$$\bar{G}_{\text{peak}} \underbrace{h\nu \left(\frac{\pi}{2} \Delta\nu \right)}_{\text{Zero point input}} = P$$

$$\underbrace{K \cdot \frac{(\Delta\nu_{\text{cc}})^2}{(\Delta\nu)^2}}_{\bar{G}_{\text{peak}}} \cdot h\nu \left(\frac{\pi}{2} \Delta\nu \right) = P \quad \longrightarrow \quad \boxed{\Delta\nu = K \frac{\frac{\pi}{2} h\nu \cdot (\Delta\nu_{\text{cc}})^2}{P}}$$

Conclusions ???

Below Threshold:

- ASE patterns are observed by spatio-spectral method.
- Patterns are very nonuniform and are not efficiently represented in terms of modes -- $\{U_n\}$, $\{V_n\}$
- Regenerative amplification of optimum input fields $\{S_n\}$ provide reasonable agreement with data
- Petermann - K appears in the gain \otimes bandwidth relationship for optimum inputs

At Threshold & Above Threshold:

- Will nonuniform mode build-up create nonuniform saturation and mode competition?
- How does one develop a proper quantum theory of a laser with an unstable resonator (Non-Hermitian Optical resonator) ?

DISTRIBUTION LIST

AUL/LSE

Bldg 1405 - 600 Chennault Circle

Maxwell AFB, AL 36112-6424 1 cy

DTIC/OCP

8527 John J. Kingman Rd, Suite 0944

Ft Belvoir, VA 22060-6218 2 cys

AFSAA/SAI

1580 Air Force Pentagon

Washington, DC 20330-1580 1 cy

PL/SUL

Kirtland AFB, NM 87117-5776 2 cys

PL/HO

Kirtland AFB, NM 87117-5776 1 cy

Official Record Copy

PL/LIDA/Depatie 4cy

PL/VT

Al Paxton

Kirtland AFB, NM 87117-5776 1 cy

PL/LIDA

Greg Dente

Kirtland AFB, NM 87117-5776 1 cy

Dr Ted Salvi

Logicon R D A

2600 Yale Blvd, SE

Albuquerque, NM 87106 1 cy